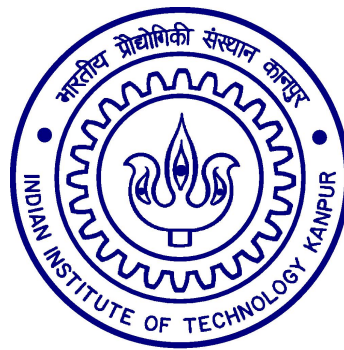


Constitutive modelling of Rubber-like material

A thesis submitted
in partial fulfillment of the requirements
for the Degree of
Master of Technology

by
SIDDHARTHA SRIVASTAVA



to the
Department of Aerospace Engineering
INDIAN INSTITUTE OF TECHNOLOGY KANPUR
Kanpur, INDIA - 208016
July 2015

Dedicated to my parents

Certificate

This is to certify that the work contained in the thesis titled “**Constitutive modelling of Rubber-like material**”, by Siddhartha Srivastava (Roll No. 10327715), has been carried out under my supervision for the partial fulfillment of masters degree in the Department of Aerospace Engineering, IIT Kanpur and this work has not been submitted elsewhere for any other degree.

Prof. C.S.Upadhyay

Professor

July 2015

Department of Aerospace Engineering

Indian Institute of Technology Kanpur

Kanpur, INDIA - 208016

Acknowledgement

I find myself blessed to have spent such a wonderful time in this institute. I am equally fortunate to find this opportunity to express my gratitude to everyone who has been an integral part of this journey.

Firstly I would like to express my sincere gratitude to my supervisor Dr. C.S. Upadhyay. His patient guidance and encouragement kept me motivated at all times. The discussions and meetings we had were a great intellectual and learning experience for me. I am indebted to him.

The knowledge I gained through the courses by Dr. S Das, Dr. S Basu, Dr. S Mahesh and Dr. S Chakrobarthy is a cornerstone for this thesis. I am also thankful to Dr Abhishek and Dr. Mathpal for their continuous guidance and encouragement.

I would like to thank my classmates Deo, Rana, Dwivedi, Suchandra and Verma for being the stress relievers as they were. I would also like to thank them for the wonderful discussions we had on topics way beyond the monotony of a single thesis. I would also like to thank all my colleagues at *Structural Analysis Lab* particularly Koley and Babu for helping me throughout my stay in the research group. I would also like to thank my other friends especially Anurag, Harsh, Kuldeep, Nagesh, Rawat, Sagar, Shashank, Shashwat and Yash for making my stay in this campus a memorable one.

Lastly, I would like to express my gratitude to my parents and brother for their unparalleled support and encouragement. They have always been an *oasis of serenity* in my expeditions.

Abstract

A significant amount of literature is dedicated for understanding the behavior of rubber-like materials. These effectively non-compressible materials exhibit non-linear as well as history dependent behavior. Another behavior observed in these materials is the damage induced stress softening also known as Mullin's effect. These materials are heavily utilized in industry due to their ability to sustain large deformation. Due to this, the constitutive law is required to realistically model the behavior of material for as high as 500% strain and should contain minimal material parameters.

In this work a new damaged visco-elastic plastic model is proposed. Its efficacy is demonstrated for experimental results of rubber under large strain. An invariant based hyperelastic continuum model is used for capturing the non-linear behaviour. The rate dependent stress-strain behavior of these elastomeric materials is known to exhibit hysteresis upon cyclic loading due to viscous effect. The viscous effects are included in the model by considering two interacting networks of state dependent and rate dependent networks contributing to equilibrium and non-equilibrium energy respectively. The model further demonstrates Mullins effect by incorporating an isotropic continuum damage parameter. The model is capable of capturing material behavior under different general multiaxial loading conditions.

Contents

Abstract	ix
1 Introduction	1
1.1 Motivation	1
1.2 Literature Review	4
1.3 Thesis Outline	5
2 Continuum Mechanics and Thermodynamics	7
2.1 Introduction	7
2.2 Kinematics	7
2.2.1 Gradient, Divergences and Time derivatives	9
2.2.2 Deformation Gradient	10
2.2.3 Volumetric changes	10
2.2.4 Polar Decomposition	11
2.2.5 Spectral decomposition	12
2.2.6 Strains	12
2.2.7 The Velocity gradient	13
2.3 Small deformation approximation	14
2.3.1 Infinitesimal strain	14
2.3.2 Volumetric changes in small deformation	15
2.4 Forces and Stresses	15
2.4.1 Axiom of momentum balance	15
2.4.2 Traction	16

2.4.3	Hydrostatic and Deviatoric stress	16
2.4.4	Other measures of stress	17
2.5	Thermodynamics	18
2.5.1	First Principle	19
2.5.2	Second Principle	19
2.5.3	Claussius-Duhem inequality	19
3	Constitutive Modelling	21
3.1	Introduction	21
3.2	Constitutive Theory	21
3.2.1	Axioms	21
3.2.2	Simplifications	23
3.3	Case Study: Damaged Viscoelastic Plastic model	24
3.3.1	Mathematical Formulation	24
4	Model reduction and Implementation	31
4.1	Introduction	31
4.2	Hyperelastic form	31
4.2.1	Incompressibility constraint	32
4.3	Reduced 1D Model	32
4.3.1	Simple axial loading	33
4.3.2	Reduced evolution equation	33
4.4	Numerical Implementation	34
4.5	Results and Discussion	34
4.5.1	Non-linear behaviour	34
4.5.2	Case: Monotonic Loading	35
4.5.3	Case: Cyclic Loading	36
4.5.4	Case: Segment-wise loading	37
5	Conclusion	47
5.1	Scope for future work	47

5.1.1	Increasing the active range of viscous effects	47
5.1.2	Rate independent non-virgin hysteresis	47
A	Thermodynamics and Constitutive theory	49
A.1	Claussius-Duhem Inequality	49
A.1.1	Derivation	49
A.2	Objectivity of rate of deformation tensor	50
B	Mathematical Identities	51
B.1	Useful derivatives	51
B.2	Some properties related to internal product	52
B.3	Symmetries in fourth order tensors	52
B.3.1	Isotropic tensors	53

List of Figures

1.1	Strain rate effect on Natural rubber material in monotonic loading for different strain rates (Ref. Khan (2015))	2
1.2	Scanning Electron Microscopy of EPDM rubber material with a loaded cracktip (Ref. Khan (2015))	2
1.3	Mechanical behavior of rubber under cyclic loading [see Khan (2015)]	3
1.4	Molecular-level observation of fillers and polymers comprising tire compounds Toyo (2015)	3
3.1	1-D illustration of a generalized Maxwell model for viscoelastic material	28
4.1	Stress-Stretch curve for the Ogden hyperelastic material with parameters shown in Table 4.1	35
4.2	Stretch vs Time curve for a monotonic loading case with strain rate $= 0.2s^{-1}$	36
4.3	Stress-Stretch curve for a monotonic loading case with strain rate $= 0.2s^{-1}$ (parameters shown in Table 4.1 and 4.2)	37
4.4	Damage evolution in material for a monotonic loading case with strain rate $= 0.2s^{-1}$ (parameters shown in Table 4.1 and 4.2))	38
4.5	Inelastic evolution in material for a monotonic loading case with strain rate $= 0.2s^{-1}$ (parameters shown in Table 4.1 and 4.2))	39
4.6	Comparision of Stretch-Stress curves for material in monotonic loading with different strain rates (parameters shown in Table 4.1 and 4.2))	39

4.7	Stretch vs Time curve for a cyclic loading case (3 cycles) with strain rate = $0.2s^{-1}$	40
4.8	Stress-Stretch curve for a cyclic loading case (3 cycles) with strain rate = $0.2s^{-1}$ (parameters shown in Table 4.1 and 4.2)	40
4.9	Damage evolution in material for a cyclic loading case (3 cycles) with strain rate = $0.2s^{-1}$ (parameters shown in Table 4.1 and 4.2))	41
4.10	Inelastic evolution in material for a cyclic loading case (3 cycles) with strain rate = $0.2s^{-1}$ (parameters shown in Table 4.1 and 4.2))	41
4.11	Stretch vs Time curve for a segment-wise cyclic loading case (9 cycles)	42
4.12	Stress-Stretch curve for a segment-wise cyclic loading case (9 cycles) without viscous effects (parameters shown in Table 4.1 and 4.3)	42
4.13	Damage evolution in material for a segment-wise cyclic loading case (9 cycles) without viscous effects (parameters shown in Table 4.1 and 4.3))	43
4.14	Inelastic evolution in material for a segment-wise cyclic loading case (9 cycles) without viscous effects (parameters shown in Table 4.1 and 4.3))	43
4.15	Stress-Stretch curve for a segment-wise cyclic loading case (9 cycles) with strain rate = $0.2s^{-1}$ (parameters shown in Table 4.1 and 4.2)	44
4.16	Damage evolution in material for a segment-wise cyclic loading case (9 cycles) with strain rate = $0.2s^{-1}$ (parameters shown in Table 4.1 and 4.2))	44
4.17	Inelastic evolution in material for a segment-wise cyclic loading case (9 cycles) with strain rate = $0.2s^{-1}$ (parameters shown in Table 4.1 and 4.2))	45
4.18	Q (Viscous branch) evolution in material for a segment-wise cyclic loading case (9 cycles) with strain rate = $0.2s^{-1}$ (parameters shown in Table 4.1 and 4.2))	45

5.1 Comparison of hysteresis in Natural rubber for different strain rates
(Ref. Khan (2015)) 48

Chapter 1

Introduction

Rubber and rubber-like materials are of prime importance in industrial fields of Aerospace, Civil, Mechanical as well as rapidly emerging Biomedical Engineering. Some practical applications may include tires and tubes industry which is the largest consumer of rubber in terms of quantity. Other examples are elastomeric bearings, used for earthquake load isolation which uses alternating layer of rubber and steel. The debonding of these layers is one of the many problems that warrant active research in the constitutive modelling of rubber and rubber like materials. The human soft tissue behaves very similarly to rubber material and thus can be modelled similarly. The elasticity of rubber is nonlinear and modelling its mechanical properties has always been a big challenge.

1.1 Motivation

Mechanical behavior of rubber material is recognized to be nonlinear visco-elastic. Figure 1.1 shows the stress-strain behaviour of natural rubber at different strain rates. In addition, cyclic loading experiments have shown existence of inelastic dissipation in the form of equilibrium hysteresis and a *permanent set*. This dissipation is often attributed to damage growth mechanisms in material, for instance, void growth at high strains. Figure 1.2 shows growth of microscale voids in front of a loaded cracktip in EPDM material. This permanent set often appears as residual

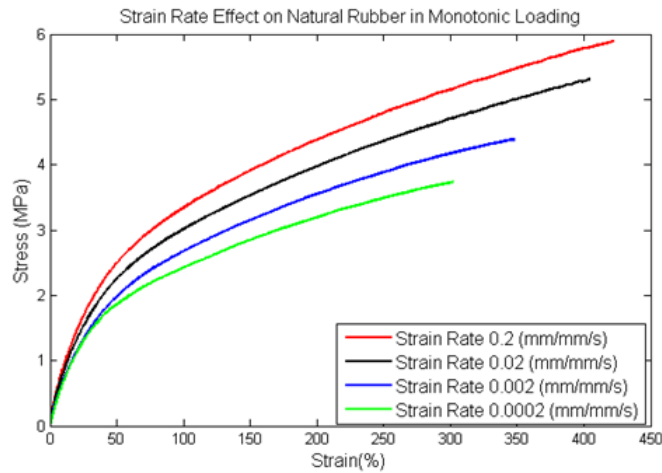


Figure 1.1: Strain rate effect on Natural rubber material in monotonic loading for different strain rates (Ref. Khan (2015))

strain in the literature but nevertheless is a well accepted jargon in rubber industry. Another characteristic feature evident in these materials is the phenomenon of *Mullins Effect* (proposed in Mullins (1948)), which is characterized by the stress softening in the first few loading cycles while finally approaching towards a stable hysteresis loop. Experimental results for a cyclic loading is shown in figure 1.3. It can be seen that the virgin curve (first cycle in each segment) almost envelopes the consecutive cycles. In addition to hysteresis in first cycle we also see hysteresis in consecutive cycles with almost like limit cycle response. Residual strain also increases with each segment. The above mentioned phenomenon is attributed to

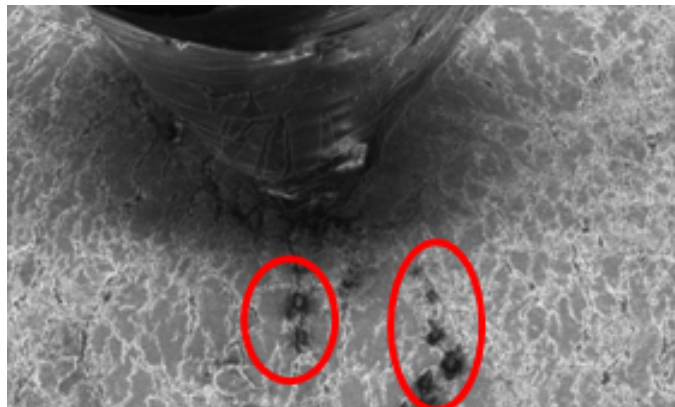


Figure 1.2: Scanning Electron Microscopy of EPDM rubber material with a loaded cracktip (Ref. Khan (2015))

multiscale effects at micro and meso levels (see illustration in figure 1.4). These

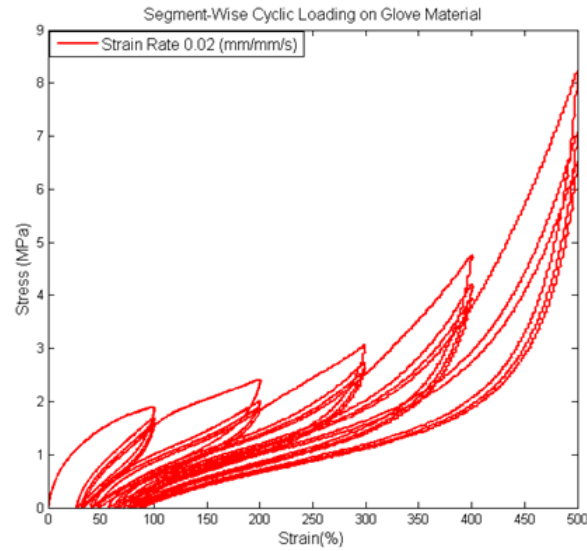


Figure 1.3: Mechanical behavior of rubber under cyclic loading [see Khan (2015)]

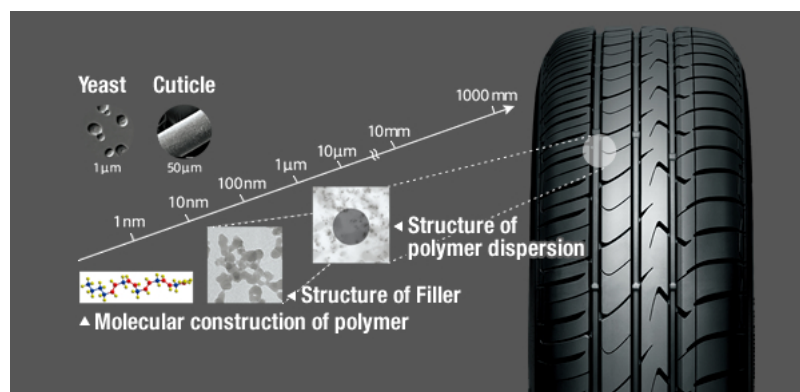


Figure 1.4: Molecular-level observation of fillers and polymers comprising tire compounds Toyo (2015)

materials generally have added impurities for tailoring their mechanical properties like strength and fatigue life etc. These filler particles interact with the matrix (Rubber) introducing complex thermo-mechanical responses. Another complexity is added at the meso-scale due to the interaction of molecular chains present in the matrix. The slipping, entanglement and de-entanglement of chains causes energy losses and storage resulting in interesting macro-scale responses. These behavioural attributes together form a platform for mathematically rich constitutive modelling.

1.2 Literature Review

The theory of finite strain non-linear elasticity, particularly the incompressible theory has been widely used to model the non-linear mechanical response of rubber-like materials. The idea is centered on finding a strain energy density as a function of stress or strain and finding the derivative as the respective work conjugates. Popular strain energy functions derived through purely continuum approach are due to Mooney (1940), Rivlin (1948) and Ogden (1972). These functions have also been derived by employing statistical mechanics on the underlying structure of rubber as in Arruda and Boyce (1993). But since these are conservative energy functions they do not capture any viscous effect, Mullins effect or residual strains. Much work is employed on modelling the Mullins effect (proposed in Mullins (1948)). This effect was explained in Mullins and Tobin (1957) and Mullins (1969) by proposing existence of rubber in a bi-phasic state particularly in hard and soft phases where the initial hard phase would convert to soft phase on loading. They modelled this using a damage parameter of strain amplification factor in the hard phase. This approach was widely used, for instance, in Harwood and Payne (1966a,b); Bueche (1961); Beatty and Krishnaswamy (2000). A particularly interesting article is due to Sodhani and Reese (2014) where they use a micromechanical approach to distinguish between bound (elasto-plastic) and matrix (hyper-elastic) phase of material using change in glass transition temperature near the filler particles.

Another popular approach to model these phenomenon is the concept of *Pseudo-elasticity*. In this phenomenological approach a continuous damage parameter is incorporated into the theory of quasi-static elasticity. Ogden and Roxburgh (1999) introduced stress softening but without considerations of residual strain and non virgin hysteresis (hysteresis in consecutive cycles). This issue of non-virgin hysteresis was resolved in Dorfmann and Ogden (2003) and the issue of residual strain was resolved in Dorfmann and Ogden (2004).

Strain induced crystallization is an interesting phenomenon seen in rubbers which possess regular and oriented polymer chains. The phenomenon refers to formation

of crystalline structures on mechanical loading like fibrillar structures (Mandelkern (1964)), thin lamella-like plates (Germer and Storks (1938); Keller (1957); Flory (1962)), or both resulting in *Shish-Kebab structures*. Recent work by Dargazany et al. (2014) provides an excellent review of the concerned literature.

But in the author's knowledge all the above models consider only quasi-static loading and thus do not explain the viscous effects. Purely phenomenological approaches have also provided competent and generic models. Visco-elastic models like Reese and Govindjee (1998); Bergström and Boyce (1998) offer good emulation of strain rate effects studied experimentally but fail to capture residual strain and stress softening. To incorporate the effect of stress softening, many damaged visco-elastic models have emerged (see for e.g. Simo (1987); Kaliske et al. (2001)). These models efficiently capture the experimental data for monotonic as well as cyclic loading, but they do not provide limiting permanent strain which can be seen in samples left for long periods after stretching and releasing Khan (2015). To capture this effect, plasticity was added to these models (see representative work by Lion (1996); Miehe and Keck (2000)). These damaged visco-elastic plastic models prove very effective in capturing all the aspects of rubber elasticity but at the same time increased the parameter space of the model.

1.3 Thesis Outline

In Chapter 2, the theory of continuum mechanics and thermodynamics is reviewed. In Chapter 3, first the basic concepts of constitutive modelling are stated and then a damaged visco-elastic plastic model is formulated. In Chapter 4, the model is reduced for a uniaxial case and a numerical implementation scheme is discussed. At the same time qualitative behavior of the uniaxial model is compared with the experimental results. Finally conclusions along with suggestion for future work are given in Chapter 5.

Chapter 2

Continuum Mechanics and Thermodynamics

2.1 Introduction

This chapter reviews the basic concepts of mechanics and thermodynamics in continuous media. The definitions and notations employed in this chapter are used throughout the subsequent chapters of this thesis. For a more in-depth study of the subject the reader is referred to the excellent literature presented in books by Lemaitre and Chaboche (1994); Maugin (1992); Gross and Seelig (2011); de Souza Neto et al. (2011)

2.2 Kinematics

Let B be a body which occupies an open region Ω of a 3D Euclidean space E with a regular boundary $\partial\Omega$ in its reference configuration. A deformation of B is defined by a smooth one to one mapping of a point P on reference configuration of B to deformed configuration of B

$$\Phi : \Omega \rightarrow E \tag{2.1}$$

$$x = \Phi(P) \tag{2.2}$$

where the deformed configuration will be denoted by $\Phi(\Omega)$.

The displacement field $u(P)$ is defined as

$$u(P) = \Phi(P) - P \quad (2.3)$$

Rigid deformation is defined as a deformation which preserves the distance between all material points and can be represented as a combination of rotation and translation. In rigid translation, the displacement field is a constant and given by

$$\Phi(P) = P + u \quad (2.4)$$

In rigid rotation the displacement field is a constant and given by

$$\Phi(P) = \Phi(Q) + R(P - Q) \quad (2.5)$$

where Q is the point about which the body is rotated and R is a proper orthogonal rotation matrix. Motion of B refers to a time-dependent deformation of B defined by the function

$$\Phi : \Omega \times t \rightarrow E \quad (2.6)$$

i.e. the map $\Phi(., t)$ is a deformation of B for each time t .

During the motion the material velocity of a particle is defined as

$$\dot{x}(P, t) = \frac{\partial \Phi(P, t)}{\partial t} \quad (2.7)$$

Since the map Φ is invertible, material points can be expressed in terms of their location at time t as

$$P = \Phi^{-1}(x, t) = x - u(\Phi^{-1}(x, t), t) \quad (2.8)$$

Φ^{-1} is called the reference map and can be used to define the spatial velocity field of a material particle at (x,t) as

$$v(x, t) \equiv \dot{x}(\Phi^{-1}(x, t), t) \quad (2.9)$$

The concept of material and spatial velocity field can be extended to a general field. A general time-dependent (scalar, vector or tensor) field defined over body B can be categorized as material or spatial field. If the field is expressed as a function of material particles P and time t i.e. its domain is $\Omega \times t$ then the field is said to be a material field whereas if its domain is $\Phi(\Omega, t) \times t$ then the field is said to be a spatial field.

2.2.1 Gradient, Divergences and Time derivatives

The material and spatial gradients of a field α denoted respectively by $\nabla_P \alpha$ and $\nabla_x \alpha$ are given as

$$\nabla_P \alpha = \frac{\partial \alpha_m(P, t)}{\partial P} \quad (2.10)$$

$$\nabla_x \alpha = \frac{\partial \alpha_s(x, t)}{\partial x} \quad (2.11)$$

Similarly the material and spatial time derivatives of α denoted respectively by $\dot{\alpha}$ and α' are given as

$$\dot{\alpha} = \frac{\partial \alpha_m(P, t)}{\partial t} \quad (2.12)$$

$$\alpha' = \frac{\partial \alpha_s(x, t)}{\partial t} \quad (2.13)$$

The definitions of gradients can be used to define spatial and material divergences of vector field \mathbf{v} as

$$div_P \mathbf{v} = trace(\nabla_P \mathbf{v}) \quad (2.14)$$

$$div_x \mathbf{v} = trace(\nabla_x \mathbf{v}) \quad (2.15)$$

For a tensor field \mathbf{T} , the divergences can be compactly defined, in cartesian components as

$$(\operatorname{div}_P \mathbf{T})_i = \frac{\partial \mathbf{T}_{ij}}{\partial P_j} \quad (2.16)$$

$$(\operatorname{div}_x \mathbf{T})_i = \frac{\partial \mathbf{T}_{ij}}{\partial x_j} \quad (2.17)$$

2.2.2 Deformation Gradient

The deformation gradient, \mathbf{F} of a deformation is a second order tensor defined as

$$\mathbf{F}(P, t) = \nabla_P \Phi(P, t) = \frac{\partial x_i}{\partial P} \quad (2.18)$$

which can be rewritten using equation 2.4 as

$$\mathbf{F} = \mathbf{I} + \nabla_P u \quad (2.19)$$

The cartesian component of \mathbf{F} are given as

$$F_{ij} = \delta_{ij} + \frac{\partial u_i}{\partial P_j} \quad (2.20)$$

2.2.3 Volumetric changes

Consider an infinitesimal volume dV_0 defined in reference configuration. The mapping of this volume in the deformed configuration is given as dV . The volume of these two elements are related through following identity

$$\det \mathbf{F} = \frac{dV}{dV_0} \quad (2.21)$$

It should be noted that the body is not allow to penetrate itself thus constraining J to be a positive real quantity.

Any deformation can be locally decomposed as a purely volumetric deformation (contractions/dilations) and an isochoric deformation (volume preserving). This

can be represented using multiplicative split of deformation gradient as

$$\mathbf{F} = \mathbf{F}_{iso}\mathbf{F}_v \quad (2.22)$$

where the isochoric component is given by

$$\mathbf{F}_{iso} = (\det\mathbf{F})^{-1/3}\mathbf{F} \quad (2.23)$$

and the volumetric component is

$$\mathbf{F}_v = (\det\mathbf{F})^{1/3}\mathbf{I} \quad (2.24)$$

2.2.4 Polar Decomposition

A polar decomposition refers to locally decomposing a deformation into a rotation tensor and a symmetric positive definite tensor. This can be represented as

$$\mathbf{F} = \mathbf{R}\mathbf{U} = \mathbf{V}\mathbf{R} \quad (2.25)$$

where \mathbf{R} is the orthogonal rotation tensor and \mathbf{U} and \mathbf{V} are, respectively, the right and left stretch tensor. The stretch tensor can be related by the following identity

$$\mathbf{V} = \mathbf{R}\mathbf{U}\mathbf{R}^T \quad (2.26)$$

The stretch tensors can also be expressed, respectively, in terms of right and left *Cauchy-Green strain tensors*

$$\mathbf{U} = \sqrt{\mathbf{C}} \quad (2.27)$$

$$\mathbf{V} = \sqrt{\mathbf{B}} \quad (2.28)$$

Using the property of orthogonality of rotation tensor, the *Cauchy-Green strain tensors* can be given as

$$\mathbf{C} = \mathbf{U}^2 = \mathbf{F}^T \mathbf{F} \quad (2.29)$$

$$\mathbf{B} = \mathbf{V}^2 = \mathbf{F} \mathbf{F}^T \quad (2.30)$$

2.2.5 Spectral decomposition

Since \mathbf{U} and \mathbf{V} are symmetric they admit spectral decomposition which is given by

$$\mathbf{U} = \sum_1^3 \lambda_i \mathbf{l}_i \otimes \mathbf{l}_i \quad (2.31)$$

$$\mathbf{V} = \sum_1^3 \lambda_i \mathbf{e}_i \otimes \mathbf{e}_i \quad (2.32)$$

where the $\{\lambda_i\}$ are the principal stretches, and the orthogonal triads $\{\mathbf{l}_i\}$ and $\{\mathbf{e}_i\}$ are respectively, the *Lagrangian and Eulerian triads* related by

$$\mathbf{l}_i = R \mathbf{e}_i \quad (2.33)$$

2.2.6 Strains

Let us consider dp , a small vector in the undeformed space and its mapping dx in the deformed space related as $dx = \mathbf{F} dp$. Therefore, the deformed length is given by

$$\|dx\|^2 = \mathbf{F} dp \cdot \mathbf{F} dp = \mathbf{C} \|dp\|^2 = \left(I + 2\mathbf{E}^{(2)} \right) \|dp\|^2 \quad (2.34)$$

where $\mathbf{E}^{(2)}$ is the so called *Green-Lagrange strain tensor* given as

$$\mathbf{E}^{(2)} = \frac{1}{2} (\mathbf{C} - I) = \frac{1}{2} \left[\nabla_P u + (\nabla_P u)^T + (\nabla_P u)^T \nabla_P u \right] \quad (2.35)$$

Also note that the eigenvectors of $\mathbf{E}^{(2)}$ coincide with the Lagrange triad, therefore it can also be expressed as

$$\mathbf{E}^{(2)} = \sum_1^3 \frac{1}{2} (\lambda_i^2 - 1) \mathbf{l}_i \otimes \mathbf{l}_i \quad (2.36)$$

This property of Lagrangian triad gives birth to a family of *Lagrangian strain tensors* given as

$$\mathbf{E}^{(n)} = \begin{cases} \frac{1}{n} (\mathbf{U}^n - \mathbf{1}) & : n \neq 0 \\ \log \mathbf{U} & : n = 0 \end{cases} \quad (2.37)$$

where n is any real number. In spectral space this can be represented as following

$$\mathbf{E}^{(n)} = \sum_1^3 g(\lambda_i) \mathbf{l}_i \otimes \mathbf{l}_i \quad (2.38)$$

where

$$g(\lambda_i) = \begin{cases} \frac{1}{n} (\lambda_i^n - 1) & : n \neq 0 \\ \log \lambda_i & : n = 0 \end{cases} \quad (2.39)$$

Some other popular members of this family are the Biot ($n = 1$), Hencky ($n = 0$) and Almansi ($n = -2$) strain tensors. Analogous to this one can define a *family of Eulerian strain tensor*.

2.2.7 The Velocity gradient

The velocity gradient is a spatial gradient field (discussed in 2.2.1 on page 9) given as

$$\mathbf{L} = \nabla_x \mathbf{v} = \frac{\partial}{\partial t} \left(\frac{\partial \Phi}{\partial P} \right) \frac{\partial P}{\partial x} = \dot{\mathbf{F}} \mathbf{F}^{-1} \quad (2.40)$$

\mathbf{L} can be further split into rate of deformation tensor, \mathbf{D} (also referred as stretching tensor) and the spin tensor \mathbf{W}

$$\mathbf{D} = \text{symmetric}(\mathbf{L}), \quad \mathbf{W} = \text{skew}(\mathbf{L}) \quad (2.41)$$

The *volume change rate*, \dot{J} is given as

$$\dot{J} = J \text{trace}(\mathbf{D}) = J \text{div}_x \mathbf{v} \quad (2.42)$$

2.3 Small deformation approximation

When the deformation gradient is sufficiently small, certain simplifications can be made in the kinematic description.

2.3.1 Infinitesimal strain

Cauchy green strain tensor for a finite deformation can be given, in terms of displacement as

$$\mathbf{C} = I + \nabla_P u + (\nabla_P u)^T + (\nabla_P u)^T \nabla_P u \quad (2.43)$$

$$\mathbf{B} = I + \nabla_P u + (\nabla_P u)^T + \nabla_P u (\nabla_P u)^T \quad (2.44)$$

For sufficiently small value of $\nabla_P u$ this can be approximated to

$$\mathbf{C} \equiv \mathbf{B} \equiv I + \nabla_P u + (\nabla_P u)^T \quad (2.45)$$

Therefore the *Green-Lagrange strain tensor* can be given as,

$$\mathbf{E}^{(2)} \equiv \epsilon = \frac{1}{2} \left[\nabla_P u + (\nabla_P u)^T \right] \quad (2.46)$$

where ϵ is called as infinitesimal strain tensor. Analogous to 2.34 the deformed length for infinitesimal deformation is given by

$$\|dx^2\| = (I + 2\epsilon) \|dp^2\| \quad (2.47)$$

2.3.2 Volumetric changes in small deformation

In contrast to multiplicative split of F in finite deformations, the infinitesimal strain tensor can be approximated using an additive split. The resulting isochoric and volumetric strain for small deformation can be given by

$$\epsilon = \epsilon_V + \epsilon_{iso} \quad (2.48)$$

where,

$$\epsilon_V = \frac{1}{3} \text{trace}(\nabla u) I = \frac{1}{3} I \otimes I : \epsilon \quad (2.49)$$

$$\epsilon_{iso} = \left(I_S - \frac{1}{3} I \otimes I \right) : \epsilon \quad (2.50)$$

See appendix B.3.1 for the definitions of these tensors.

2.4 Forces and Stresses

In real bodies forces are transmitted through molecular interaction. In the regime of continuum mechanics we talk about forces in average sense and this assumption is valid for length scales much greater than atomic scale.

2.4.1 Axiom of momentum balance

The axiom of momentum balance asserts that for any part \mathcal{P} of the deformed configuration of body B with boundary S , the balance of linear momentum and angular momentum are satisfied, these are given by

Linear Momentum

$$\int_{\partial\mathcal{P}} t(n) da + \int_{\mathcal{P}} \rho b dv = \int_{\mathcal{P}} \rho \dot{\mathbf{v}} dv \quad (2.51)$$

Angular Momentum

$$\int_{\partial\mathcal{P}} x \times t(n) da + \int_{\mathcal{P}} \rho x \times b dv = \int_{\mathcal{P}} \rho x \times \dot{\mathbf{v}} dv \quad (2.52)$$

where $t(n)$ and b are spatial fields of traction and body forces acting on a deformed body B with $\partial\mathcal{P}$ as an arbitrarily oriented smooth surface with normal n .

2.4.2 Traction

Traction vector is the force (per unit area) exerted by material on one side of an arbitrary surface (inside the body) to the other side. Central to continuum mechanics is the concept of Cauchy stress tensor which is defined as the traction vector which measures force exerted across material surface per unit *deformed area*. In accordance with Cauchy's theorem which establishes linear dependence of normal (n) on traction (t), we define the very famous 2nd order tensor: Cauchy stress tensor given as

$$t(x, n) = \sigma(x)n \quad (2.53)$$

Moreover, Cauchy stress tensor is symmetric i.e. $\sigma = \sigma^T$ and therefore admits spectral representation given as

$$\sigma = \sum \sigma_i e_i^* \otimes e_i^* \quad (2.54)$$

where the eigenvalues σ_i are called the principal Cauchy stress and eigenvectors e_i^* are called the principal stress direction.

2.4.3 Hydrostatic and Deviatoric stress

In constitutive modelling it is often convenient to split Cauchy stress into mean(pI) and deviatoric(s) components given as

$$\sigma = s + pI \quad (2.55)$$

where

$$s = \left(I_S - \frac{1}{3} I \otimes I \right) : \sigma \quad (2.56)$$

$$pI = \frac{1}{3} I \otimes I : \sigma \quad (2.57)$$

See appendix B.3.1 for the definitions of these tensors.

2.4.4 Other measures of stress

It is often convenient to define other stress measures since in general we do not have knowledge of the deformed surface a priori. These lead to the definition of stress measures like First Piola-Kirchhoff stress, Second Piola-Kirchhoff stress and Kirchhoff stress.

First Piola-Kirchhoff stress

The tensor S^{PK1} is called the first Piola-Kirchhoff stress and is often referred to as the Piola-Kirchhoff stress or nominal stress. It is given as

$$S^{PK1} = J \sigma F^{-T} \quad (2.58)$$

with the corresponding traction vector given as

$$t_0 = \sigma^{PK1} m \quad (2.59)$$

where m is the normal to surface $\partial \mathcal{P}$ in the reference frame. Please note that the traction calculated here is the force per unit undeformed area. It can also be shown that S^{PK1} is generally not symmetric (a property that we would like to have). This leads to the definition of Second Piola-Kirchhoff stress

Second Piola-Kirchhoff stress

The Second Piola-Kirchhoff is given as

$$S^{PK2} = JF^{-1}\sigma F^{-T} \quad (2.60)$$

It is trivial to see that symmetry of σ implies symmetry of S^{PK2} .

Kirchhoff stress

Another important measure of stress is the Kirchhoff stress tensor, τ , defined by

$$\tau = J\sigma \quad (2.61)$$

Due to the symmetry of σ , the Kirchhoff stress is symmetric.

2.5 Thermodynamics

Let us first introduce some scalars: Temperature(T), specific internal energy(e), specific entropy(s) and density of heat production(r) to understand the fundamentals of thermodynamics. Additionally, vector fields \mathbf{b} and \mathbf{q} will represent the body force and heat flux respectively. All definitions are in deformed configuration. Next we will introduce fundamental conservation laws of mass and momentum.

The postulate of conservation of mass states

$$\dot{\rho} + \rho \operatorname{div}_x \dot{\mathbf{u}} = 0 \quad (2.62)$$

The conservation of momentum states, in spatial configuration,

$$\operatorname{div}_x \sigma + \mathbf{b} = \rho \ddot{\mathbf{u}} \quad \text{in } \Phi(\Omega) \quad (2.63)$$

$$t = \sigma n \quad \text{in } \Phi(\partial\Omega)$$

In the material configuration it can be restated as

$$\begin{aligned} \operatorname{div}_P S^{PK1} + \mathbf{b}_0 &= \rho_0 \ddot{\mathbf{u}} \quad \text{in } \Omega \\ t_0 &= S^{PK1} m \quad \text{in } \partial\Omega \end{aligned} \quad (2.64)$$

where

$$\mathbf{b}_0 = J\mathbf{b} \quad (2.65)$$

$$\rho_0 = J\rho \quad (2.66)$$

2.5.1 First Principle

The first principle of thermodynamics postulates the conservation of energy and is given as

$$\rho \dot{e} = \sigma : D + \rho r - \operatorname{div}_x \mathbf{q} \quad (2.67)$$

2.5.2 Second Principle

The second principle of thermodynamics postulates the irreversibility of entropy given as

$$\rho \dot{s} + \operatorname{div}_x \left[\frac{\mathbf{q}}{\theta} \right] - \frac{\rho r}{\theta} \geq 0 \quad (2.68)$$

2.5.3 Claussius-Duhem inequality

From first and second principle of thermodynamics it follows that

$$\rho \dot{s} + \operatorname{div}_x \left[\frac{\mathbf{q}}{\theta} \right] - \frac{1}{\theta} (\rho \dot{e} - \sigma : D + \operatorname{div}_x \mathbf{q}) \geq 0 \quad (2.69)$$

Let us introduce an energy form called *Helmholtz energy*, defined as

$$\bar{\Psi} = e - \theta s \quad (2.70)$$

On substituting Helmholtz energy form in equation 2.69 and carrying on straight forward algebra we get the spatial form of *Claussius-Duhem inequality* given as,

$$\sigma : D - \rho \left(\dot{\Psi} + s\dot{\theta} \right) - \frac{1}{\theta} \mathbf{q} \cdot \nabla_x \theta \geq 0 \quad (2.71)$$

It can be restated in material form as

$$\tau : D - \rho_0 \left(\dot{\Psi} + s\dot{\theta} \right) - \frac{J}{\theta} \mathbf{q} \cdot \nabla_P \theta F^{-1} \geq 0 \quad (2.72)$$

Note that the left side of the Eq.2.71 and 2.72 represents the dissipation in deformed and reference configuration respectively.

In the next chapter we will apply this theory to develop a constitutive model and we will also look into the axioms of constitutive theory.

Chapter 3

Constitutive Modelling

3.1 Introduction

In Chapter 2, we discussed the basic principles valid for all continuum materials. In this chapter, we will first briefly look into the *Constitutive theory* and then develop a simplified visco-elastic plastic model for finite strains to simulate rubber elasticity.

3.2 Constitutive Theory

We are interested in global macroscopic behavior of materials, which can be modelled phenomenologically by a constitutive model. In this section we will discuss the theory for developing such *constitutive models*, to differentiate between different type of continuum materials. For completeness, let us first define the rules (axioms) central to this theory.

3.2.1 Axioms

Determinism

The axiom of material determinism states that the history of independent constitutive state (e.g. strain, temperature) variable determines the present dependent state (e.g. stress, change in entropy) i.e. if ξ represents set of all independent state

variable and Ξ represents the set of all the dependent state variable then

$$\Xi(t) = \Pi(\xi^t) \quad (3.1)$$

where $(.)^t$ represent the time history of the quantity.

Memory

The axiom of memory states that the values of the independent states at distant past do not affect the dependent variables as appreciably as the ones in near past.

Equipresence

The axiom of equipresence states that at the outset all constitutive functionals must be expressed in terms of same list of independent variable. Although some of these variables can be eliminated using assumptions and approximations.

Local action

The axiom of local action states that the values of independent variables at distant spatial point from x do not affect the dependent variable at x as appreciably as the ones in neighbourhood. Although in this thesis, we will only work in the regime of local theories where this axiom is trivially satisfied.

Objectivity

The axiom of objectivity states that constitutive equations must be form-invariant with respect to spatial frame of reference. Form-invariance requires deformation gradient F to be transformed on rigid rotation Q in the following way

$$F^* = QF \quad (3.2)$$

Scalar fields are unaffected by change of frame but tensors like Cauchy stress σ change according to the following rule,

$$\sigma^* = Q\sigma Q^T \quad (3.3)$$

while vectors like heat flux q transform according to the following rule,

$$q^* = Qq \quad (3.4)$$

Admissibility

The axiom of admissibility states that all constitutive equations must be consistent with the laws of thermodynamics given in section 2.5

3.2.2 Simplifications

In addition to the rules mentioned in section 3.2.1, certain simplifications can be made to the constitutive law. These simplifications still result in a general class of materials.

Symmetry Groups

Symmetry groups are a set of density preserving changes of reference configuration under which the set of all material response functionals (Π) are not affected. The symmetry group for solids is a subset of proper orthogonal group, i.e. set of all rotations. A material is said to be isotropic if the symmetry group is the entire proper orthogonal group.

Internal State Variables

The constitutive equation written in history form as in equation 3.1 is far too general to be of any practical utility. An effective alternate to the general description based on the history is the adoption of *thermodynamics with internal variables*. It

hypothesize that at any point of time in a thermodynamic process, the thermodynamic state is completely defined by the instantaneous values of a finite number of state variables. The thermodynamic state is independent of the history of these state variables.

3.3 Case Study: Damaged Viscoelastic Plastic model

In this section, although simple linear evolution laws are taken in this model, the modular structure presented here can be used to include non-linear evolution as well.

3.3.1 Mathematical Formulation

Let us start by assuming that the deformation admits a multiplicative distribution of elastic and inelastic component of deformation given as

$$F = F_e F_i \quad (3.5)$$

Substituting this to the definition of *Right Cauchy Green tensor* given as

$$C_j = F_j^T F_j \quad (3.6)$$

where $j = e, i$

we get,

$$C = F_i^T C_e F_i \quad (3.7)$$

Energy Form

Let us take an ansatz of **Helmholtz Energy form** as:

$$\Psi = (1 - D) \Psi^0(C_e) + \Psi^v(C_e, Q) + \Psi^I \quad (3.8)$$

This energy form is motivated by the form taken in Simo (1987). Here Ψ^0 , Ψ^v and Ψ^I represent the elastic, viscous and inelastic energy forms respectively. Q represents a generic *internal state variable* and D *damage state variable* where $D \subset [0, 1]$ with $D = 0$ being the undamaged state.

The choices of Ψ^v and Ψ^I for this energy form is similar to the form of generalized Maxwell model for visco-elastic material. A brief discussion on the energy form is presented in section 3.3.1 of this chapter.

Thermodynamic admissibility

In this section we will discuss the conditions for thermodynamic admissibility of this energy form based on the axioms discussed in section 3.

We start by taking the time derivative of the energy form given in 3.8 to get,

$$\dot{\Psi} = (1 - D) \frac{\partial \Psi^0}{\partial C_e} : \dot{C}_e - \Psi^0 \dot{D} + \frac{\partial \Psi^v}{\partial C_e} : \dot{C}_e + \frac{\partial \Psi^v}{\partial Q} : \dot{Q} + \dot{\Psi}^I \quad (3.9)$$

where the equation 3.7 can be equivalently written as,

$$C_e = F_i^{-T} C F_i^{-1} \quad (3.10)$$

Taking time derivative of equation 3.10 we get,

$$\dot{C}_e = \dot{F}_i^{-T} C F_i^{-1} + F_i^{-T} \dot{C} F_i^{-1} + F_i^{-T} C \dot{F}_i^{-1} \quad (3.11)$$

Substituting equations 3.8 and 3.11 in *Claussius-Duhem inequality* (the form given in A.1) we get,

$$\begin{aligned} S^{PK2} : \dot{C} - 2\rho_0 \frac{\partial ((1 - D) \Psi^0 + \Psi^v)}{\partial C_e} : \\ \left[\dot{F}_i^{-T} C F_i^{-1} + F_i^{-T} \dot{C} F_i^{-1} + F_i^{-T} C \dot{F}_i^{-1} \right] \\ + 2\rho_0 \left[\Psi^0 \dot{D} - \frac{\partial \Psi^v}{\partial Q} \dot{Q} - \dot{\Psi}^I \right] \geq 0 \end{aligned} \quad (3.12)$$

Using identities given in appendix B.5 we can further simplify the above inequality as,

$$\begin{aligned} & \left[S^{PK2} - 2\rho_0 F_i^{-1} \frac{\partial((1-D)\Psi^0 + \Psi^v)}{\partial C_e} F_i^{-T} \right] : \dot{C} \\ & - 2\rho_0 \frac{\partial((1-D)\Psi^0 + \Psi^v)}{\partial C_e} : \left[\dot{F}_i^{-T} C F_i^{-1} + F_i^{-T} C \dot{F}_i^{-1} \right] \\ & + 2\rho_0 \left[\Psi^0 \dot{D} - \frac{\partial \Psi^v}{\partial Q} \dot{Q} - \dot{\Psi}^I \right] \geq 0 \end{aligned} \quad (3.13)$$

Here C , F_i , Q and D are the independent quantities. C can assume any real value. We can fix rate of change of F_i , Q , D to zero and vary \dot{C} . Thus for the above inequality to be true, coefficient of \dot{C} must be 0. This exercise results in a relation for S^{PK2} and dissipation(G) given as,

$$S^{PK2} = 2\rho_0 F_i^{-1} \frac{\partial((1-D)\Psi^0 + \Psi^v)}{\partial C_e} F_i^{-T} \quad (3.14)$$

$$\begin{aligned} \frac{G}{2\rho_0} = & - \frac{\partial((1-D)\Psi^0 + \Psi^v)}{\partial C_e} \left\{ \dot{F}_i^{-1} C F_i^{-T} + F_i^{-1} C \dot{F}_i^{-T} \right\} \\ & + \Psi^0 \dot{D} - \frac{\partial \Psi^v}{\partial Q} \dot{Q} - \dot{\Psi}^I \geq 0 \end{aligned} \quad (3.15)$$

The first term in dissipation inequality can be further simplified using equations 3.7 along with identities given in B.1 and B.2 as,

$$\begin{aligned} & - 2\rho_0 \frac{\partial((1-D)\Psi^0 + \Psi^v)}{\partial C_e} : \left[\dot{F}_i^{-T} C F_i^{-1} + F_i^{-T} C \dot{F}_i^{-1} \right] \\ & = F_i S^{PK2} F_i^T : F_i^{-T} \dot{F}_i^T F_i^{-T} C F_i^{-1} + F_i^{-T} C F_i^{-1} \dot{F}_i F_i^{-1} \\ & = F_i S^{PK2} F_i^T : (L_i^T C_e + C_e L_i) \end{aligned} \quad (3.16)$$

where L_i is the inelastic velocity gradient defined as,

$$L_i = \dot{F}_i F_i^{-1} \quad (3.17)$$

Now we further assume a strong form of dissipation, i.e.,

$$F_i S^{PK2} F_i^T : C_e L_i \geq 0 \quad (3.18)$$

$$\Psi^0 \dot{D} \geq 0 \quad (3.19)$$

$$\frac{\partial \Psi^v}{\partial Q} \dot{Q} + \dot{\Psi}^I \leq 0 \quad (3.20)$$

Please note that this decoupling introduces additional restrictions on the solution.

Evolution Laws

For simplicity we assume linear evolution laws for the damage and inelastic deformation given as,

$$\dot{D} = \dot{\beta} \Psi^0 \quad (3.21)$$

$$L_i = C_e^{-1} \cdot \Upsilon(\dot{\beta}) : F_i \cdot S \cdot F_i^T \quad (3.22)$$

where L_i is defined in equation 3.17, $\dot{\beta}$ is a Lagrange multiplier and Υ is a semi positive definite fourth order isotropic tensor linearly dependent on $\dot{\beta}$ containing parameters $v_1 \geq 0$ and $v_2 \geq 0$ given as

$$\Upsilon = \frac{v_1 \dot{\beta}}{3} I \otimes I + v_2 \dot{\beta} \left(I_S - \frac{1}{3} I \otimes I \right) \quad (3.23)$$

The properties of these tensors are given in appendix B.3.

At this point we would like to borrow some terms from plasticity for convenience.

First is the Yield surface defined as (see Simo (1987))

$$\Phi = \sqrt{2\Psi^0} - \sqrt{2\Psi^0}_{max} \quad (3.24)$$

Please note that we have assumed a strain surface to be the yield function which often is very convenient with Helmholtz energy formulation. The term $\sqrt{2\Psi^0}_{max}$ is related to maximum energy stored in hyperelastic branch in the deformation history.

And the other is "Loading-Unloading conditions" given as

$$\dot{\beta} > 0; \quad \Phi \leq 0; \quad \dot{\beta}\Phi = 0 \quad (3.25)$$

Please note that the linear evolution equations given in equations in 3.21 and 3.22 results in a quadratic form of dissipation. The non-negative value of \dot{D} and hyperelastic energy form Ψ^0 and semipositive definiteness of Υ results in non-negative dissipation terms. Additionally since the assumed form of L_i is symmetric (by virtue of isotropy of Υ see appendix B.3.1), this definition of L_i is equivalent to definition of rate of deformation gradient D which ensures objectivity of constitutive law (see appendix A.2).

Viscous Branch

Before formulating the finite strain viscous model let us first discuss the basic generalized Maxwell model. An illustration for the 1D case is given in figure 3.1. The

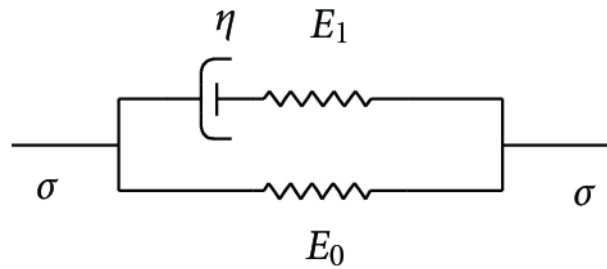


Figure 3.1: 1-D illustration of a generalized Maxwell model for viscoelastic material

energy form (for 1D case) for such a model can be given as sum of energies in all the components

$$\Psi = \underbrace{\frac{1}{2}E_0\varepsilon_0^2}_{E_0 \text{ Spring}} + \underbrace{\frac{1}{2}E_1\varepsilon_1^2}_{E_1 \text{ Spring}} + \underbrace{\int \eta \dot{\varepsilon}_2 d\varepsilon_2}_{\text{damper}} \quad (3.26)$$

where ε_0 represents the total deformation of the parallel system, ε_1 represents the deformation in E_1 spring and ε_2 is the deformation in the damper. The energy can

alternatively be represented as,

$$\begin{aligned}\Psi &= \frac{1}{2}E_0\varepsilon_0^2 + \int \sigma_1 d(\varepsilon_0 - \varepsilon_2) + \int \eta \dot{\varepsilon}_2 d\varepsilon_2 \\ &= \frac{1}{2}E_0\varepsilon_0^2 + \int \sigma_1 d(\varepsilon_0 - \varepsilon_2) + \int \eta \left(\dot{\varepsilon}_0 - \frac{\dot{\sigma}_1}{E_1}\right) \dot{\varepsilon}_2 dt\end{aligned}\quad (3.27)$$

Where σ_1 represents the stress across in both damper and E_1 spring (equilibrium condition). And all the components (spring and damper) follow linear constitutive laws.

On taking the time derivative of equation 3.27 we get the power as,

$$\begin{aligned}\dot{\Psi} &= E_0\varepsilon_0\dot{\varepsilon}_0 + \sigma_1(\dot{\varepsilon}_0 - \dot{\varepsilon}_2) + \eta\left(\dot{\varepsilon}_0 - \frac{\dot{\sigma}_1}{E_1}\right)\dot{\varepsilon}_2 \\ &= (E_0\varepsilon_0 + \sigma_1)\dot{\varepsilon}_0 + \eta\left(\dot{\varepsilon}_0 - \frac{\sigma_1}{\eta} - \frac{\dot{\sigma}_1}{E_1}\right)\dot{\varepsilon}_2\end{aligned}\quad (3.28)$$

On substituting the above equation in CD inequality given in equation 2.71 and rationalizing the non-negative dissipation as done for equation 3.13, we get,

$$\sigma = \underbrace{E_0\varepsilon_0}_{\sigma_{equilibrium}} + \underbrace{\sigma_1}_{\sigma_{non-equilibrium}} \quad (3.29)$$

$$\eta\left(\frac{\dot{\sigma}_{equilibrium}}{E_0} - \frac{\sigma_{non-equilibrium}}{\eta} - \frac{\dot{\sigma}_{non-equilibrium}}{E_1}\right)\dot{\varepsilon}_2 \geq 0 \quad (3.30)$$

Using similar argument on equation 3.30 we get the evolution law,

$$\dot{\sigma}_{non-equilibrium} = \frac{E_1\dot{\sigma}_{equilibrium}}{E_0} - \frac{E_1\sigma_{non-equilibrium}}{\eta} \quad (3.31)$$

Please note that we can also derive equation 3.31 by imposing the equilibrium condition of same stress σ_1 across damper and E_1 spring.

With this model as the basis, let us take the ansatz for the form of energy of

viscous branch as

$$\Psi^v = \int Q : dC_e - \frac{1}{2} Q : Q \quad (3.32)$$

$$\Psi^I = \zeta \int (\gamma \dot{S}^{PK2} - \dot{Q}) : dQ \quad (3.33)$$

where Q is an internal state variable which in some sense model the deformation of viscous spring. On substituting the above equations in equation 3.20 we get,

$$\zeta(\dot{Q} - \gamma \dot{S}^{PK2} + \frac{1}{\zeta} Q) \dot{Q} \geq 0 \quad (3.34)$$

We also see that Q appears in the overstress term in the in S^{PK2} .

Let us now constraint the energy to a form where the coefficient of $\dot{Q} = 0$, this leads to the evolution equation as

$$\dot{Q} = \gamma \dot{S}^{PK2} - \frac{1}{\zeta} Q \quad (3.35)$$

Please note that at constant strain rate $\dot{Q} = 0$ as $t \rightarrow \infty$

The analytical solution to the above equation is given by the hereditary integral

$$Q = \gamma \int_0^t \exp^{\frac{s-t}{\tau}} \frac{\partial S^{PK2}(s)}{\partial s} ds \quad (3.36)$$

In this chapter we reviewed the constitutive theory and developed a 3-D damaged viscoelastic plastic model. In the next chapter we will reduce the model for uniaxial case and implement it in a MATLAB code to see its qualitative behaviour.

Chapter 4

Model reduction and Implementation

4.1 Introduction

In Chapter 3, we discussed the constitutive theory. In this chapter, we will first reduce the developed visco-elastic plastic model for finite strains to uniaxial case and then develop a framework for its computational implementation.

4.2 Hyperelastic form

We would first like to assume a hyperelastic model for modelling the non-linear response of material. We chose a regularised Ogden type material law (ref: Ogden (1972)). The energy function of such materials are given by

$$\rho_0 \Psi^0 (\lambda_{e(1)}^*, \lambda_{e(2)}^*, \lambda_{e(3)}^*) = \sum_{p=1}^N \frac{\mu_p}{\alpha_p} \left(\lambda_{e(1)}^{*\alpha_p} + \lambda_{e(2)}^{*\alpha_p} + \lambda_{e(3)}^{*\alpha_p} - 3 \right) + \frac{1}{2} K \log (J_e^2) \quad (4.1)$$

where J is the determinant of the deformation gradient and λ_i^* are the eigenvalues of the isochoric stretch tensor given by

$$\lambda_{e(k)}^* = \frac{\lambda_{e(k)}}{J_e^{\frac{1}{3}}} \quad (4.2)$$

Kirchhoff stress is given in terms of Ψ^0 as,

$$\tau_{(i)} = \lambda_{e(i)} \rho_0 \frac{\partial \Psi^0}{\partial \lambda_{e(i)}} \quad (4.3)$$

where no summation is implied on the repeated indices.

Consequently the Kirchhoff stress obtained by substituting energy form given in equation 4.1 in the above equation we get,

$$\tau_{(i)} = \sum_{p=1}^N \mu_p J_e^{-\alpha_p/3} \left[\lambda_{e(i)}^{\alpha_p} - \frac{1}{3} \left(\lambda_{e(1)}^{\alpha_p} + \lambda_{e(2)}^{\alpha_p} + \lambda_{e(3)}^{\alpha_p} \right) \right] + K \log J_e \quad (4.4)$$

4.2.1 Incompressibility constraint

As discussed earlier, rubber-like materials are generally incompressible. Thus there is a constraint on $\{\lambda_i\}$ given as

$$\lambda_1 \lambda_2 \lambda_3 = 1 \quad (4.5)$$

The Kirchhoff stress for this case can then be given as,

$$\tau_{(i)} = \lambda_{e(i)} \rho_0 \frac{\partial \Psi^0}{\partial \lambda_{e(i)}} - p \quad (4.6)$$

where p is a Lagrange multiplier associated with the incompressibility constraint.

It can be eliminated by using the following technique

$$\tau_{(1)} - \tau_{(3)} = \lambda_{e(1)} \rho_0 \frac{\partial \Psi^0}{\partial \lambda_{e(1)}} - \lambda_{e(3)} \rho_0 \frac{\partial \Psi^0}{\partial \lambda_{e(3)}} \quad (4.7)$$

$$\tau_{(2)} - \tau_{(3)} = \lambda_{e(2)} \rho_0 \frac{\partial \Psi^0}{\partial \lambda_{e(2)}} - \lambda_{e(3)} \rho_0 \frac{\partial \Psi^0}{\partial \lambda_{e(3)}} \quad (4.8)$$

4.3 Reduced 1D Model

Let us assume that we are interested in the 1 direction response of the material without loss of generality.

4.3.1 Simple axial loading

For a simple axial case we may take

$$\tau_2 = \tau_3 = 0 \quad (4.9)$$

We can also write $\lambda_1 = \lambda$ so that

$$\lambda_2 = \lambda_3 = \frac{1}{\lambda^{\frac{1}{2}}} \quad (4.10)$$

The implication of no transverse stress condition along with evolution equation given in equation 3.22 is that there is no inelastic growth in 2 and 3 direction. Similar arguments can be made for evolution of Q

4.3.2 Reduced evolution equation

Just like the deformation gradient (F), λ also assumes multiplicative decomposition given as,

$$\lambda = \lambda_e \lambda_i \quad (4.11)$$

The evolution equations can then be reduced to following 1-D form given as

$$\dot{\lambda}_i = c_1 \dot{\beta} S \frac{\lambda_i^3}{\lambda_e^2} \quad (4.12)$$

$$\dot{D} = c_2 \dot{\beta} \quad (4.13)$$

$$\dot{\beta} = \sqrt{2\Psi^0}_{max} \quad (4.14)$$

$$\dot{q} = \gamma \dot{S} - \frac{q}{\zeta} \quad (4.15)$$

where S and q represents the (1,1) component of S^{PK2} and Q tensor respectively.

Also note that 1-D evolution equation of λ_i contains only 1 parameter. This is due to our assumption of no Poisson type term.

4.4 Numerical Implementation

This section treats the algorithmic counterpart of the constitutive model. We consider now an algorithmic setting within a typical time interval $\Delta t = t_{n+1} - t_n$. In this small interval Δt , the evolution terms given in equations 4.12, 4.13 and 4.14 are given as,

$$\lambda_i^{(n+1)} = \lambda_i^{(n)} + c_1 \Delta \beta S \frac{\lambda_i^{(n)5}}{\lambda^{(n+1)2}} \quad (4.16)$$

$$D^{(n+1)} = D^{(n)} + c_2 \Delta \beta \quad (4.17)$$

$$\Delta \beta = \begin{cases} 0 & \text{if } \Psi_{max}^{(n+1)} \leq \Psi_{max}^{(n)} \\ \sqrt{2\Psi_{max}^{(n+1)}} - \sqrt{2\Psi_{max}^{(n)}} & \text{if } \Psi_{max}^{(n+1)} > \Psi_{max}^{(n)} \end{cases} \quad (4.18)$$

Additionally, the viscous evolution can be given as (see Kaliske et al. (2001)),

$$q^{(n+1)} = q^{(n)} \exp\left(\frac{\Delta t}{\zeta}\right) + \frac{\gamma \zeta}{\Delta t} \left(1 - \exp\left(\frac{\Delta t}{\zeta}\right)\right) \quad (4.19)$$

These equations are iteratively solved to get the final solution.

4.5 Results and Discussion

In this section we will discuss the qualitative behavior of the proposed model.

4.5.1 Non-linear behaviour

We will first look at the hyperelastic response of the Ogden material assumed for modelling the non-linear behavior of rubber. We start by assuming by material parameters which we took from Dorfmann and Ogden (2004) for a preliminary analysis. These parameters are given in Table 4.1.

μ_1	α_1	μ_2	α_2	μ_3	α_3
-1.528380	-1.011467	0.222564	4.2047799	-1.13418E-3	-4.398598

Table 4.1: Material parameters for Ogden type hyperelastic material

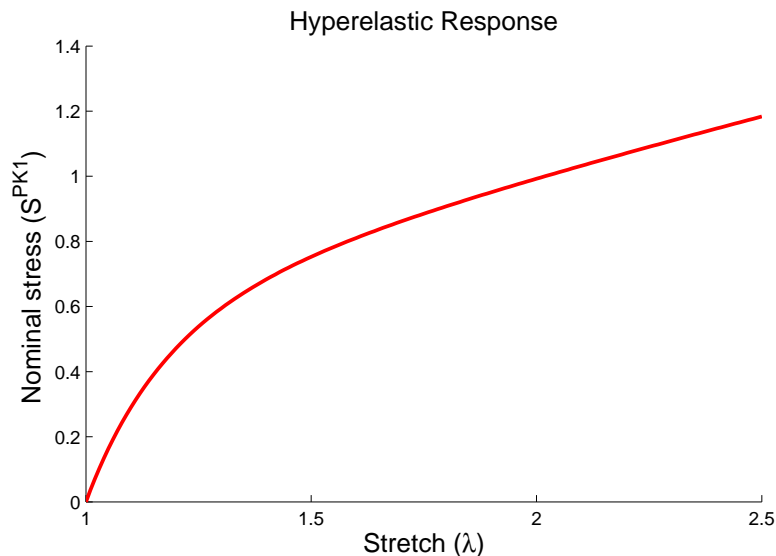


Figure 4.1: Stress-Stretch curve for the Ogden hyperelastic material with parameters shown in Table 4.1

4.5.2 Case: Monotonic Loading

In this section results for a monotonic tensile loading case for strain rate = 0.2mm/mm-sec . The stretch-time curve is shown in figure 4.2. Results are presented for upto 120% strain. Variation of Nominal stress with stretch for material parameters given in tables 4.1 and 4.2 is presented in figure4.3. The consequent damage and inelastic evolutions are given in figures 4.4 and 4.5. It can be seen that there is more than 25% damage at the maximum stretch for this choice of parameters. A similar ratio for the inelastic strain to the total strain is also observed.

Inelasticity	Damage	Viscous	
c_1	c_2	γ	ζ
0.011404	0.127093	0.1	2

Table 4.2: Material parameters for inelastic, damage and viscous branch

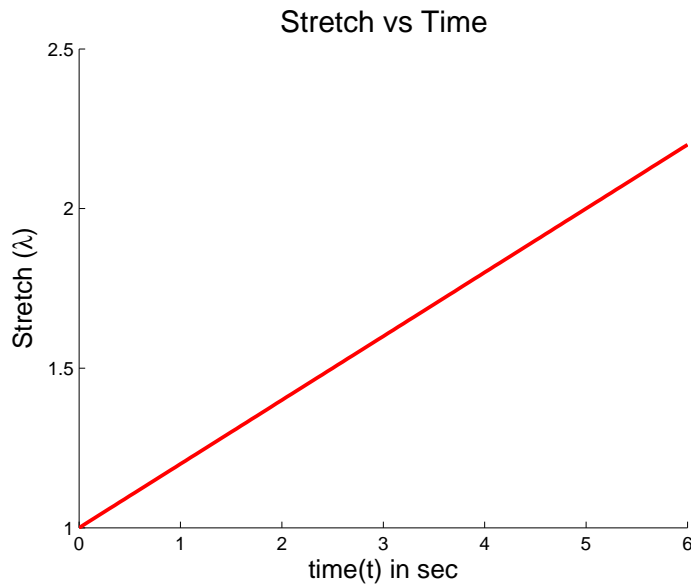


Figure 4.2: Stretch vs Time curve for a monotonic loading case with strain rate = $0.2s^{-1}$

Viscous effects

In this section we will look at the variation of stress at different strain rates. Figure 4.6 shows stress vs stretch curve for strain rates = 0.02, 0.05, 0.1, 0.2, $0.4mm/mm-sec^{-1}$. As expected, stress increases with increasing strain rate. The qualitative behaviour of all curves is similar

4.5.3 Case: Cyclic Loading

In this section we will look at the results of material response for parameters given in Table 4.1 and 4.2 for a cyclic sawtooth loading at strain rate = $0.2mm/mm-sec$. The stretch-time curve is given in figure 4.7. The stress-stretch curve shown in figure 4.8 shows existence of both virgin and non-virgin hysteresis discussed at the onset of this thesis. Although it should be noted that the hysteresis in the consecutive cycles is only due to viscous effects. Damage evolution is shown in figure 4.9. It can be seen that the damage only evolves during the first cycle. Similar result is presented for the inelastic evolution in figure 4.10.

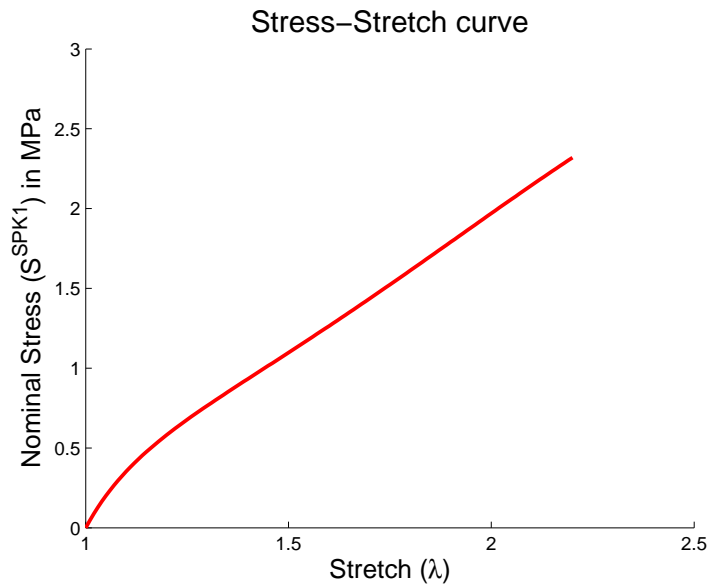


Figure 4.3: Stress-Stretch curve for a monotonic loading case with strain rate = $0.2s^{-1}$ (parameters shown in Table 4.1 and 4.2)

Inelasticity	Damage	Viscous	
c_1	c_2	γ	ζ
0.011404	0.127093	0	0

Table 4.3: Material parameters for inelasticity and damage for ideal Mullin's effect case

4.5.4 Case: Segment-wise loading

In this section we will look at the segment-wise sawtooth loading case. The stretch-time curve is given in figure 4.11 for strain rate= $0.2mm/mm - sec$. Results are presented for both non-viscous material with parameters shown in table 4.3 and viscous effect with parameters shown in table 4.2.

Without Viscous effects

The stress-stretch curve shown in figure 4.12 shows no non-virgin hysteresis. This is referred to in literature as *ideal Mullin's effect*. The stress softening and inelastic strain evolution is still evident. This can be verified by figures 4.13 and 4.14. It can also be seen that the damage and inelastic growth only occurs when the maximum strain on the material is increased. This is coherent with our expectation.

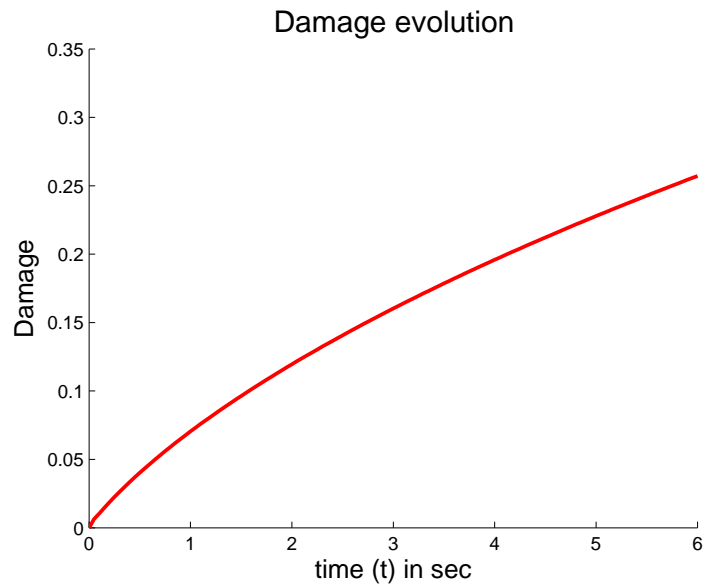


Figure 4.4: Damage evolution in material for a monotonic loading case with strain rate = $0.2s^{-1}$ (parameters shown in Table 4.1 and 4.2))

With Viscous effects

In contrast to figure 4.12, non-virgin hysteresis is present in this case as shown in the stress-stretch curve given in figure 4.15. The evolution of damage and inelastic stretch is similar to the one discussed in non-viscous case. A peculiar result can be seen in the evolution of q shown in figure 4.18. In the last segment, q assumes an increased maximum value in the consecutive cycles. This can be explained through 4.15 where \dot{q} depends directly on the rate of change of equilibrium stress. As the non-virgin curve sees a higher slope due to Mullin's effect, stress rate in consecutive cycles can be higher than the virgin cycle. This results in a slight overstress in the stress-stretch curve.

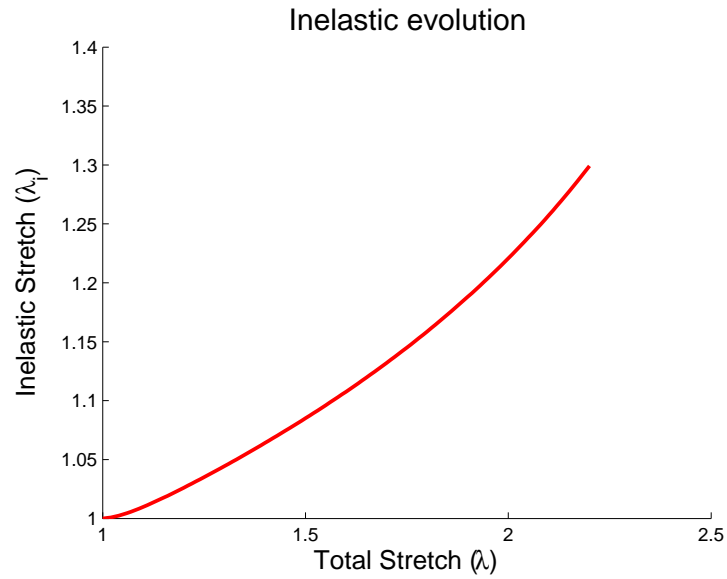


Figure 4.5: Inelastic evolution in material for a monotonic loading case with strain rate = 0.2s^{-1} (parameters shown in Table 4.1 and 4.2))

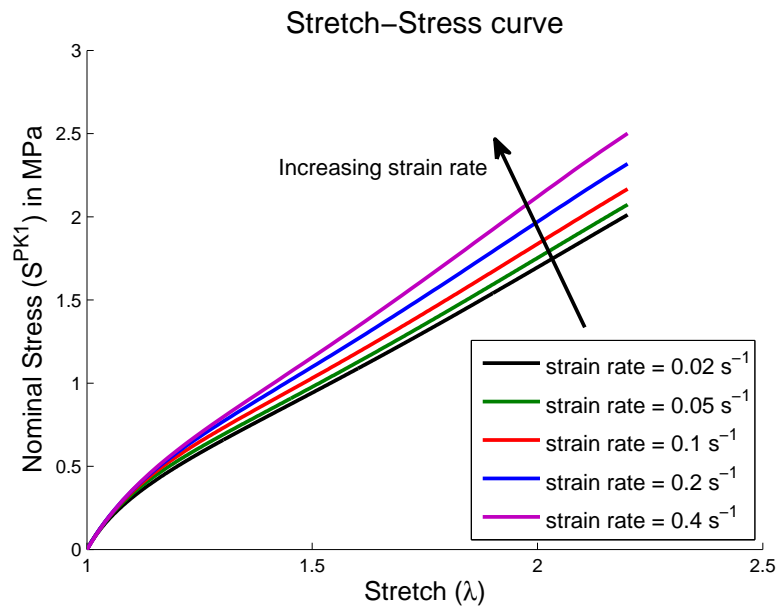


Figure 4.6: Comparison of Stretch-Stress curves for material in monotonic loading with different strain rates (parameters shown in Table 4.1 and 4.2))

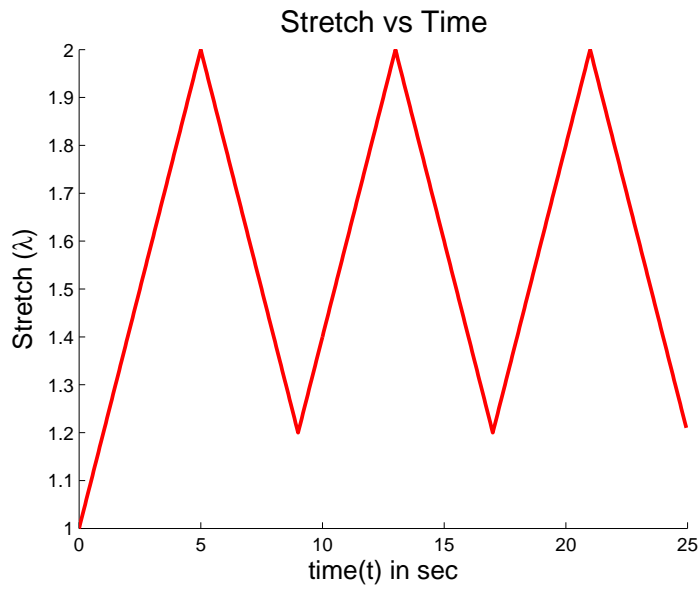


Figure 4.7: Stretch vs Time curve for a cyclic loading case (3 cycles) with strain rate = $0.2s^{-1}$

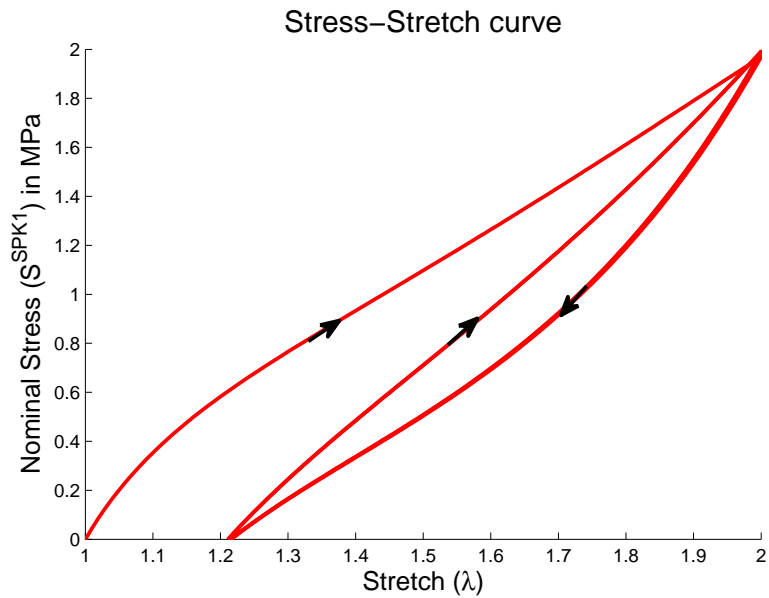


Figure 4.8: Stress-Stretch curve for a cyclic loading case (3 cycles) with strain rate = $0.2s^{-1}$ (parameters shown in Table 4.1 and 4.2)

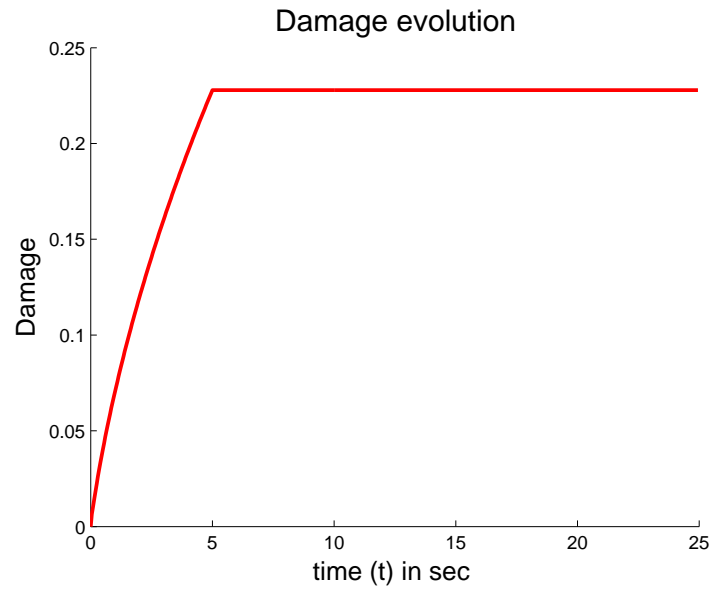


Figure 4.9: Damage evolution in material for a cyclic loading case (3 cycles) with strain rate = $0.2s^{-1}$ (parameters shown in Table 4.1 and 4.2))

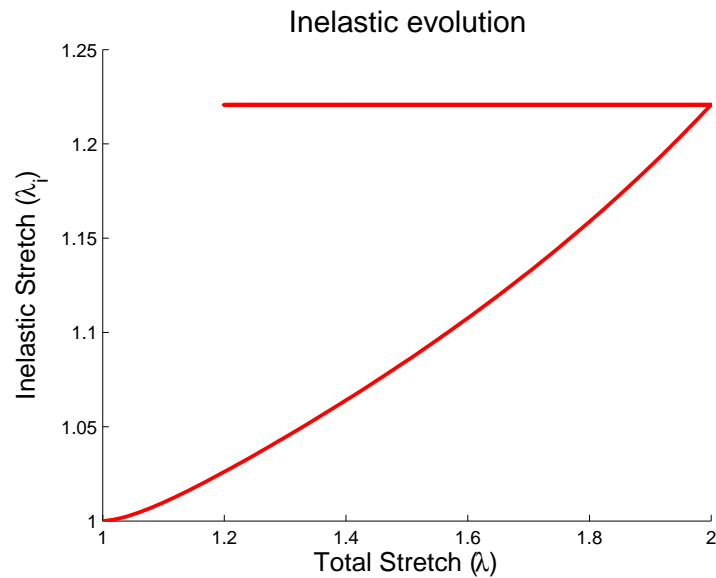


Figure 4.10: Inelastic evolution in material for a cyclic loading case (3 cycles) with strain rate = $0.2s^{-1}$ (parameters shown in Table 4.1 and 4.2))

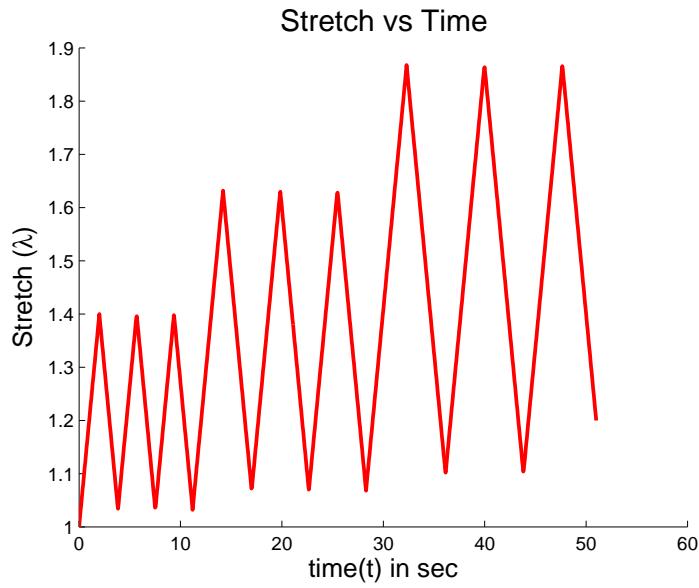


Figure 4.11: Stretch vs Time curve for a segment-wise cyclic loading case (9 cycles)

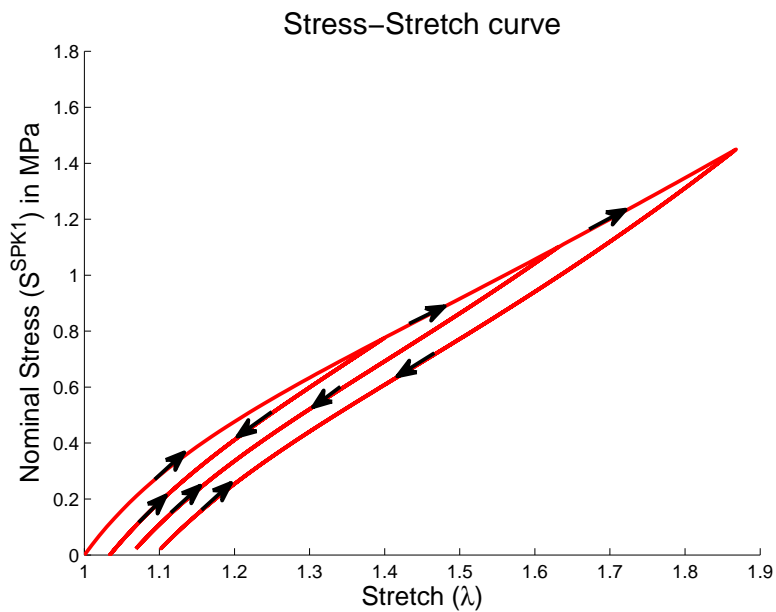


Figure 4.12: Stress-Stretch curve for a segment-wise cyclic loading case (9 cycles) without viscous effects (parameters shown in Table 4.1 and 4.3)

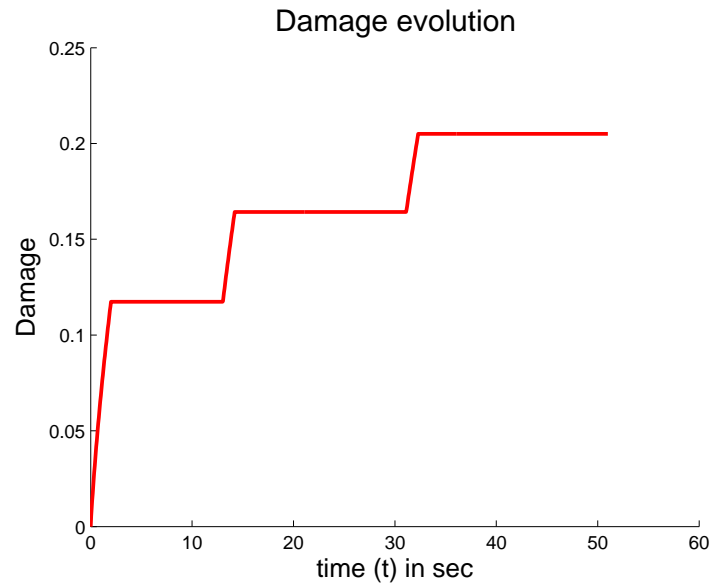


Figure 4.13: Damage evolution in material for a segment-wise cyclic loading case (9 cycles) without viscous effects (parameters shown in Table 4.1 and 4.3))

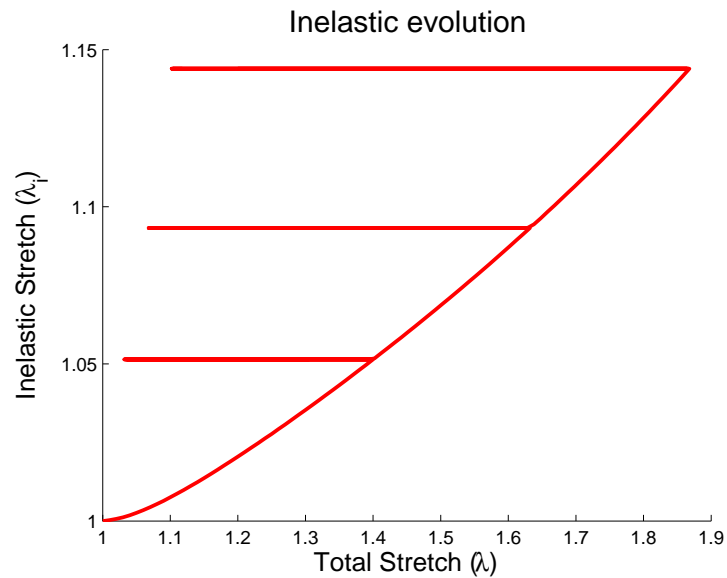


Figure 4.14: Inelastic evolution in material for a segment-wise cyclic loading case (9 cycles) without viscous effects (parameters shown in Table 4.1 and 4.3))

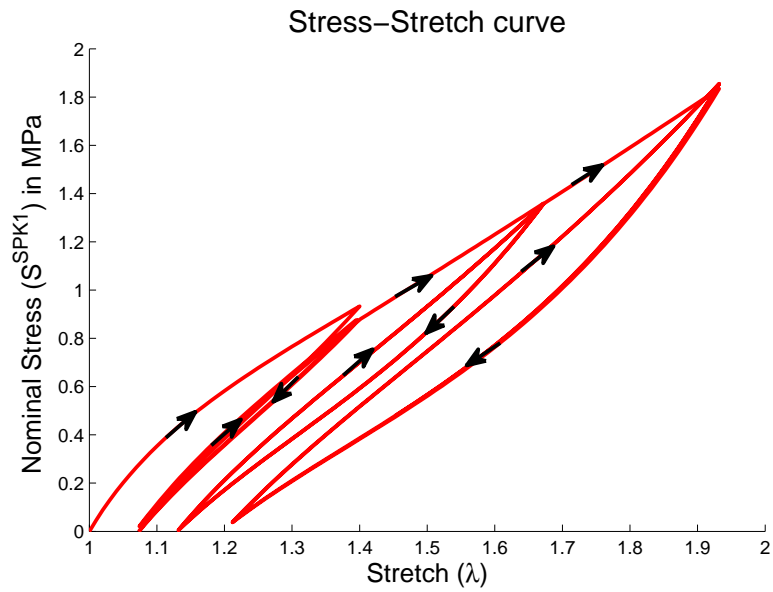


Figure 4.15: Stress–Stretch curve for a segment-wise cyclic loading case (9 cycles) with strain rate = $0.2s^{-1}$ (parameters shown in Table 4.1 and 4.2)

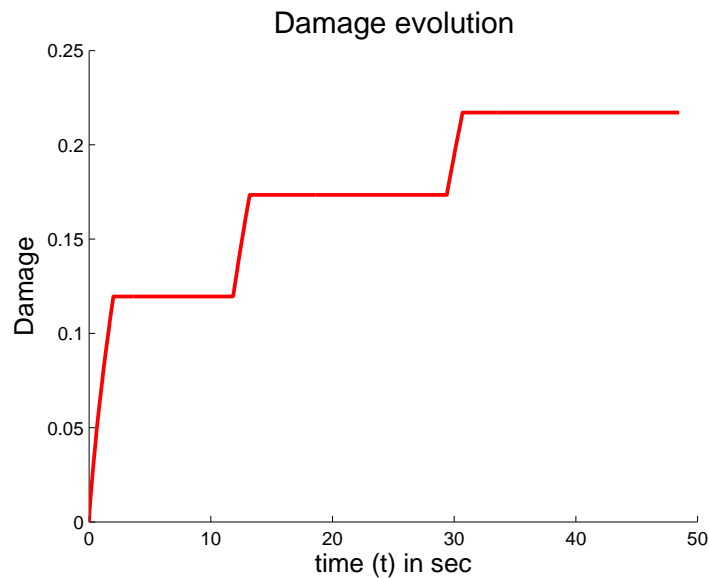


Figure 4.16: Damage evolution in material for a segment-wise cyclic loading case (9 cycles) with strain rate = $0.2s^{-1}$ (parameters shown in Table 4.1 and 4.2))

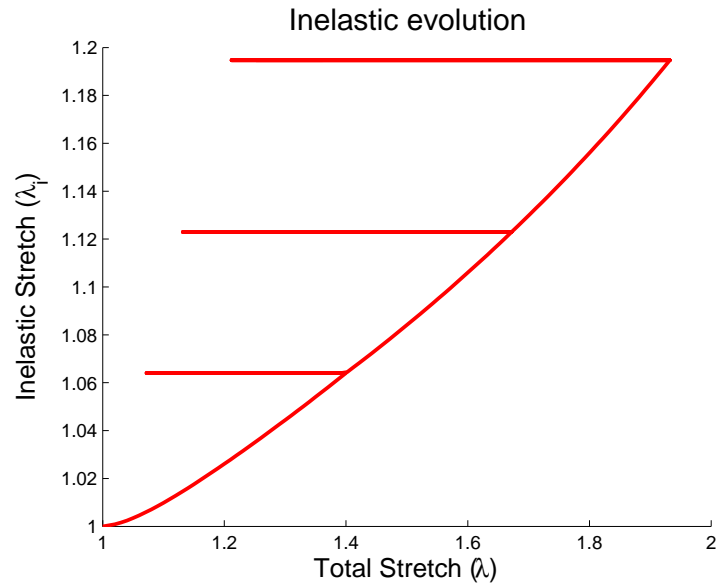


Figure 4.17: Inelastic evolution in material for a segment-wise cyclic loading case (9 cycles) with strain rate = $0.2s^{-1}$ (parameters shown in Table 4.1 and 4.2))

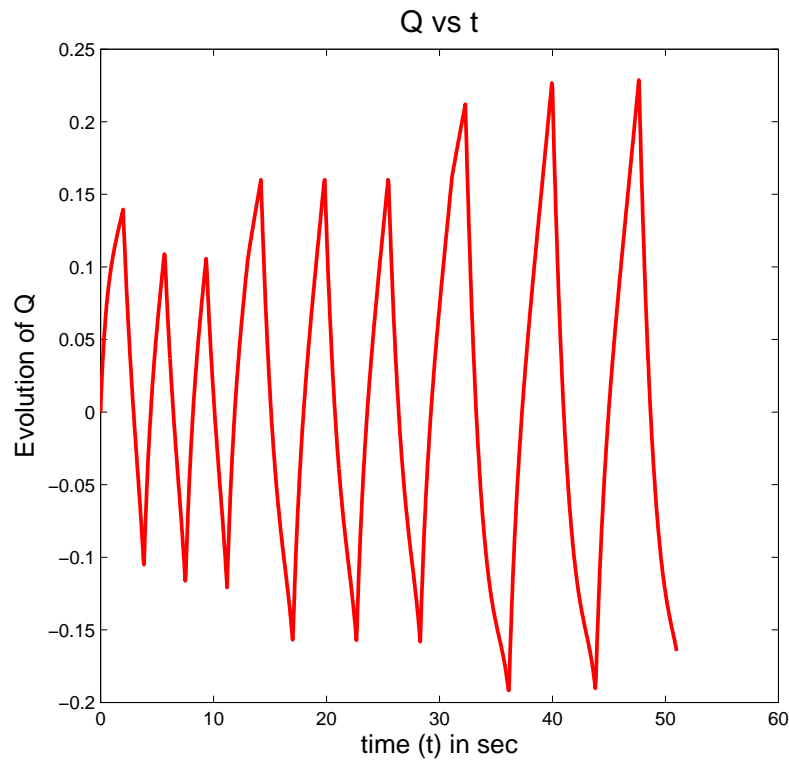


Figure 4.18: Q (Viscous branch) evolution in material for a segment-wise cyclic loading case (9 cycles) with strain rate = $0.2s^{-1}$ (parameters shown in Table 4.1 and 4.2))

Chapter 5

Conclusion

In this thesis, firstly a review of the literature and *state of the art* in modelling of rubber-like materials was presented followed by a brief overview of the basic concepts of continuum mechanics, thermodynamics and constitutive theory. A 3D damaged visco-elastic plastic model was then developed and its efficacy for modelling the mechanical behaviour of rubber was discussed. It was shown, that the model is effective for this task.

5.1 Scope for future work

5.1.1 Increasing the active range of viscous effects

Currently the model is capable of capturing strain rate effect for a range of about a single order while experimental results have shown a wider range for these effects (see figure 1.1). This problem arises due to the simplicity of the model. And the remedy is expected to be addition of extra damper-spring chains in parallel.

5.1.2 Rate independent non-virgin hysteresis

Experimental results presented in thesis by Khan (2015), show that the dissipation in non-virgin hysteresis i.e. the area in the loop is same for different strain rate. The comparison of hysteresis in Natural rubber for different strain rates is given in figure

5.1. This result does not conform with the hypothesis that the non-virgin hysteresis is solely due to viscous effect. This phenomenon warrants further research in constitutive model presented in this thesis.

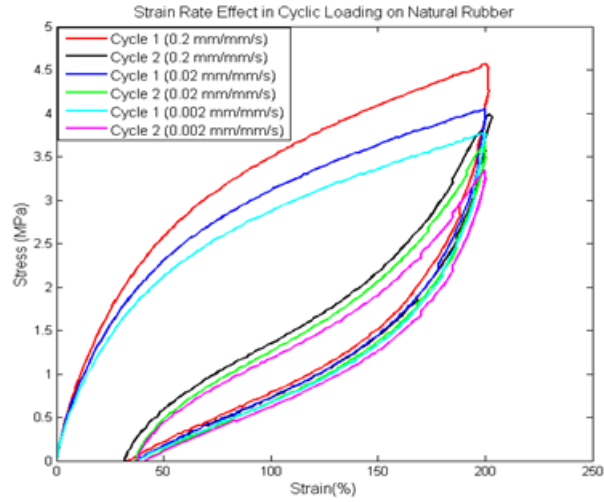


Figure 5.1: Comparison of hysteresis in Natural rubber for different strain rates (Ref. Khan (2015))

Appendix A

Thermodynamics and Constitutive theory

A.1 Claussius-Duhem Inequality

The Claussius-Duhem inequality used in chapter 3 is of the form

$$S^{PK2} : \dot{C}_e - 2\rho_0 \dot{\Psi} \geq 0 \quad (\text{A.1})$$

A.1.1 Derivation

Equation 2.72 shows the CD inequality in material frame. The first term representing the $\tau : D$ can be further modified by substituting equation 2.41, 2.40, 2.60 and 2.61

$$\begin{aligned} \tau : D &= F S^{PK2} F^T : \frac{\dot{F} F^{-1} + F^{-T} \dot{F}^T}{2} \\ &= S^{PK2} : \frac{F^T \dot{F} + \dot{F}^T F}{2} = S^{PK2} : \frac{\dot{C}_e}{2} \end{aligned} \quad (\text{A.2})$$

Substituting this in equation 2.72 and assuming isothermal conditions reduces it to equation A.1

A.2 Objectivity of rate of deformation tensor

As discussed in section 3.2.1, axiom of objectivity is one of the cornerstone of constitutive modelling. Following the same notations, we define a quantity χ for our convenience given as,

$$\chi = Q^T \dot{Q} \quad (\text{A.3})$$

It can be shown that χ is antisymmetric.

$$\frac{D}{Dt} Q^T Q = \dot{Q}^T Q + Q^T \dot{Q} = \chi^T + \chi = 0 \quad (\text{A.4})$$

In the rotated frame, the velocity gradient L^* is given as,

$$\begin{aligned} L^* &= Q(\dot{F} + \chi F)F^{-1}Q^T = Q(L + \chi)Q^T \\ &= Q(D + W + \chi)Q^T \end{aligned} \quad (\text{A.5})$$

From the antisymmetry of χ it follows that,

$$D^* = QDQ^T \quad (\text{A.6})$$

$$W^* = Q(W + \chi)Q^T \quad (\text{A.7})$$

Thus symmetric part of velocity gradient is objective.

Appendix B

Mathematical Identities

In this chapter some useful mathematical identities related to Tensors are given. These are extensively used throughout the thesis. This chapter does NOT review the topic of Tensor algebra in totality. For an indepth study, reader is referred to the books by Bowen and Wang (2008) and Bishop and Goldberg (2012)

B.1 Useful derivatives

Some of the basic expressions for derivatives of functions of vectors and tensors relevant to this thesis:

$$\frac{d\|X\|}{dX} = \frac{\|X\|}{X} \tag{B.1}$$

$$\frac{d \det(X)}{dX} = (\det(X))X^{-T} \tag{B.2}$$

$$\frac{d(X)}{dX} = I \tag{B.3}$$

$$\frac{dX^{-1}}{dt} = X^{-1} \dot{X} X^{-1} \tag{B.4}$$

B.2 Some properties related to internal product

These properties hold for any 2^{nd} order tensors R, S, t and vectors s, t, u, v

$$S : T = trace(S^T T) \quad (B.5)$$

$$I : T = trace(T) \quad (B.6)$$

$$R : (ST) = (S^T R) : T = (RT^T) : S \quad (B.7)$$

$$u \cdot Sv = S : (u \otimes v) \quad (B.8)$$

$$(s \otimes t) : (u \otimes v) = (s \cdot u)(t \cdot v) \quad (B.9)$$

$$T_{ij} = T : (e_i \otimes e_j) \quad (B.10)$$

$$(u \otimes v)_{ij} = (u \otimes v) : (e_i \otimes e_j) = u_i v_j \quad (B.11)$$

B.3 Symmetries in fourth order tensors

Any fourth-order tensors T is called symmetric if it satisfies,

$$S : T : U = (T : S) : U \quad (B.12)$$

where S, U are any second-order tensors. This symmetry is referred as major symmetry and its implication in indicial notation is given as,

$$T_{ijkl} = T_{klij} \quad (B.13)$$

Other minor symmetries are also possible in fourth-order tensors. In the case the symmetry occurs in last 2 indices, i.e. if

$$T_{ijkl} = T_{ijlk} \quad (B.14)$$

the tensor has the properties

$$T : S = T : S^T \tag{B.15}$$

$$S : T = (S : T)^T \tag{B.16}$$

If the symmetry occurs in first two indices, i.e. if

$$T_{ijkl} = T_{jikl} \tag{B.17}$$

then,

$$T : S = (T : S)^T \tag{B.18}$$

$$S : T = S^T : T \tag{B.19}$$

B.3.1 Isotropic tensors

A tensor which has the special property that its components take the same value in all Cartesian coordinate systems is called an isotropic tensor. The most general isotropic tensors of 2, 3 and 4 orders are given as $\lambda\delta_{ij}$, $\mu\epsilon_{ijk}$ and $\alpha\delta_{ik}\delta_{jl} + \beta\delta_{il}\delta_{jk} + \gamma\delta_{ij}\delta_{kl}$ where δ_{ij} and ϵ_{ijk} are the identity tensor and permutation tensor respectively and $\lambda, \mu, \alpha, \beta, \gamma$ are some scalars.

The fourth order isotropic tensor (U) can also be represented alternatively as,

$$T = \alpha\mathbf{I} + \beta I_T + \gamma(I \otimes I) \tag{B.20}$$

where α, β, γ are some scalars. Basic isotropic tensors \mathbf{I} (Fourth order identity tensor), I_T (transposition tensor) and $I \otimes I$ (tensor product of second order identity

tensors) have the following properties

$$\mathbf{I} : S = S : \mathbf{I} = S \quad (\text{B.21})$$

$$\mathbf{I} : T = T : \mathbf{I} = T \quad (\text{B.22})$$

$$I_T : S = S : I_T = S^T \quad (\text{B.23})$$

$$(I \otimes I) : T = \text{trace}(T) \quad (\text{B.24})$$

where S and T represent a generic second order and fourth order tensor.

Another basic tensor which is of importance to us is I_S which is often referred as *symmetric projection* or *symmetric identity*. It is given as,

$$I_S = \frac{1}{2}(\mathbf{I} + I_T) \quad (\text{B.25})$$

It is easy to see that it has the property,

$$I_S : S = S : I_S = \text{sym}(S) \quad (\text{B.26})$$

These generic fourth order isotropic tensors can be given in indicial notation, as,

$$\mathbf{I}_{ijkl} = \delta_{ik}\delta_{jl} \quad (\text{B.27})$$

$$(I_T)_{ijkl} = \delta_{il}\delta_{jk} \quad (\text{B.28})$$

$$(I \otimes I)_{ijkl} = \delta_{ij}\delta_{kl} \quad (\text{B.29})$$

Bibliography

- Arruda, E. M. and Boyce, M. C. (1993). A three-dimensional constitutive model for the large stretch behavior of rubber elastic materials. *Journal of the Mechanics and Physics of Solids*, 41(2):389–412.
- Beatty, M. F. and Krishnaswamy, S. (2000). A theory of stress-softening in incompressible isotropic materials. *Journal of the Mechanics and Physics of Solids*, 48(9):1931–1965.
- Bergström, J. and Boyce, M. (1998). Constitutive modeling of the large strain time-dependent behavior of elastomers. *Journal of the Mechanics and Physics of Solids*, 46(5):931–954.
- Bishop, R. L. and Goldberg, S. I. (2012). *Tensor analysis on manifolds*. Courier Corporation.
- Bowen, R. M. and Wang, C.-C. (2008). *Introduction to vectors and tensors*, volume 2. Courier Corporation.
- Bueche, F. (1961). Mullins effect and rubber–filler interaction. *Journal of applied polymer Science*, 5(15):271–281.
- Dargazany, R., Khiêm, V. N., Poshtan, E. A., and Itskov, M. (2014). Constitutive modeling of strain-induced crystallization in filled rubbers. *Physical Review E*, 89(2):022604.
- de Souza Neto, E. A., Peric, D., and Owen, D. R. J. (2011). *Computational methods for plasticity: theory and applications*. John Wiley & Sons.

- Dorfmann, A. and Ogden, R. (2003). A pseudo-elastic model for loading, partial unloading and reloading of particle-reinforced rubber. *International Journal of Solids and Structures*, 40(11):2699–2714.
- Dorfmann, A. and Ogden, R. (2004). A constitutive model for the mullins effect with permanent set in particle-reinforced rubber. *International Journal of Solids and Structures*, 41(7):1855–1878.
- Flory, P. (1962). On the morphology of the crystalline state in polymers. *Journal of the American Chemical Society*, 84(15):2857–2867.
- Germer, L. H. and Storcs, K. (1938). Arrangement of molecules in a single layer and in multiple layers. *The Journal of Chemical Physics*, 6(5):280–293.
- Gross, D. and Seelig, T. (2011). *Fracture mechanics: with an introduction to micromechanics*. Springer Science & Business Media.
- Harwood, J. and Payne, A. (1966a). Stress softening in natural rubber vulcanizates. part iii. carbon black-filled vulcanizates. *Journal of Applied Polymer Science*, 10(2):315–324.
- Harwood, J. and Payne, A. (1966b). Stress softening in natural rubber vulcanizates. part iv. unfilled vulcanizates. *Journal of Applied Polymer Science*, 10(8):1203–1211.
- Kaliske, M., Nasdala, L., and Rothert, H. (2001). On damage modelling for elastic and viscoelastic materials at large strain. *Computers & Structures*, 79(22):2133–2141.
- Keller, A. (1957). A note on single crystals in polymers: evidence for a folded chain configuration. *Philosophical Magazine*, 2(21):1171–1175.
- Khan, A. (2015). Mechanical behavior and near crack-tip deformation of rubber material: Experimental investigations and preliminary constitutive modeling.

- Lemaitre, J. and Chaboche, J.-L. (1994). *Mechanics of solid materials*. Cambridge university press.
- Lion, A. (1996). A constitutive model for carbon black filled rubber: experimental investigations and mathematical representation. *Continuum Mechanics and Thermodynamics*, 8(3):153–169.
- Mandelkern, L. (1964). *Crystallization of polymers*, volume 38. McGraw-Hill New York.
- Maugin, G. A. (1992). *The thermomechanics of plasticity and fracture*, volume 7. Cambridge University Press.
- Miehe, C. and Keck, J. (2000). Superimposed finite elastic–viscoelastic–plastoelastic stress response with damage in filled rubbery polymers. experiments, modelling and algorithmic implementation. *Journal of the Mechanics and Physics of Solids*, 48(2):323–365.
- Mooney, M. (1940). A theory of large elastic deformation. *Journal of applied physics*, 11(9):582–592.
- Mullins, L. (1948). Effect of stretching on the properties of rubber. *Rubber Chemistry and Technology*, 21(2):281–300.
- Mullins, L. (1969). Softening of rubber by deformation. *Rubber chemistry and technology*, 42(1):339–362.
- Mullins, L. and Tobin, N. (1957). Theoretical model for the elastic behavior of filler-reinforced vulcanized rubbers. *Rubber chemistry and technology*, 30(2):555–571.
- Ogden, R. (1972). Large deformation isotropic elasticity-on the correlation of theory and experiment for incompressible rubberlike solids. In *Proceedings of the Royal Society of London A: Mathematical, Physical and Engineering Sciences*, volume 326, pages 565–584. The Royal Society.

- Ogden, R. and Roxburgh, D. (1999). A pseudo-elastic model for the mullins effect in filled rubber. In *Proceedings of the Royal Society of London A: Mathematical, Physical and Engineering Sciences*, volume 455, pages 2861–2877. The Royal Society.
- Reese, S. and Govindjee, S. (1998). A theory of finite viscoelasticity and numerical aspects. *International journal of solids and structures*, 35(26):3455–3482.
- Rivlin, R. (1948). Large elastic deformations of isotropic materials. iv. further developments of the general theory. *Philosophical Transactions of the Royal Society of London A: Mathematical, Physical and Engineering Sciences*, 241(835):379–397.
- Simo, J. (1987). On a fully three-dimensional finite-strain viscoelastic damage model: formulation and computational aspects. *Computer methods in applied mechanics and engineering*, 60(2):153–173.
- Sodhani, D. and Reese, S. (2014). Finite element-based micromechanical modeling of microstructure morphology in filler-reinforced elastomer. *Macromolecules*, 47(9):3161–3169.
- Toyo (2015). Toyo tire & rubber co. ltd. <http://www.toyo-rubber.co.jp/english/rd/nano/> [Accessed: July 20, 2015].